

Stephen F. Austin State University

SFA ScholarWorks

Electronic Theses and Dissertations

Spring 5-18-2019

MOLECULAR CHARACTERIZATION OF THE PUTATIVE NUCLEOTIDE- BINDING AND HYDROLYZING ACTIVITIES OF THE ELLIS VAN CREVELD (EVC) PROTEIN

Giang Nguyen
nguyengt@jacks.sfasu.edu

Follow this and additional works at: <https://scholarworks.sfasu.edu/etds>



Part of the [Biochemistry Commons](#)

[Tell us](#) how this article helped you.

Repository Citation

Nguyen, Giang, "MOLECULAR CHARACTERIZATION OF THE PUTATIVE NUCLEOTIDE- BINDING AND HYDROLYZING ACTIVITIES OF THE ELLIS VAN CREVELD (EVC) PROTEIN" (2019). *Electronic Theses and Dissertations*. 268.

<https://scholarworks.sfasu.edu/etds/268>

This Thesis is brought to you for free and open access by SFA ScholarWorks. It has been accepted for inclusion in Electronic Theses and Dissertations by an authorized administrator of SFA ScholarWorks. For more information, please contact cdsscholarworks@sfasu.edu.

**MOLECULAR CHARACTERIZATION OF THE PUTATIVE NUCLEOTIDE- BINDING
AND HYDROLYZING ACTIVITIES OF THE ELLIS VAN CREVELD (EVC) PROTEIN**

MOLECULAR CHARACTERIZATION OF THE PUTATIVE NUCLEOTIDE-
BINDING AND HYDROLYZING ACTIVITIES OF THE ELLIS VAN CREVELD
(EVC) PROTEIN

By

GIANG THI HUONG NGUYEN, B.S. in Biotechnology

Presented to the Faculty of the Graduate School of
Stephen F. Austin State University
In Partial Fulfillment
Of the Requirements

For the Degree of
Master of Science in the Natural Sciences

STEPHEN F. AUSTIN STATE UNIVERSITY
May 2019

MOLECULAR CHARACTERIZATION OF THE PUTATIVE NUCLEOTIDE-
BINDING AND HYDROLYZING ACTIVITIES OF THE ELLIS VAN CREVELD
(EVC) PROTEIN

By

GIANG THI HUONG NGUYEN, B.S. in Biotechnology

APPROVED:

Dr. Oduyayo Odunuga, Thesis Director

Dr. Michele Harris, Committee member

Dr. Matibur Zamadar, Committee member

Dr. Rebecca Parr, Committee member

Pauline M. Sampson, Ph.D.
Dean of Research and Graduate Studies

ABSTRACT

Ellis–van Creveld (EvC) syndrome is a rare autosomal recessive disorder that is characterized by short-limb dwarfism, extra fingers or toes, malformed teeth and nails, and congenital heart defects. Mutations in two genes, EVC and EVC2, which are located on chromosome 4, have been shown to be responsible for EvC syndrome. The protein products of these genes, EVC and EVC2 physically interact and together, they are tethered to the base of the primary cilium of cells. This multi-protein assembly positively regulates the Sonic and Indian hedgehog signaling pathways by promoting downstream processes after activation of the smoothed receptor (Smo), by the hedgehog proteins. Bioinformatic analysis revealed the presence of several structural motifs in EVC sequences including P-loop, leucine zipper, transmembrane domain, and nuclear localization signal. The putative nucleotide-binding and hydrolyzing activities of EVC were tested using fragments of the protein from mice and human that contain the P-loop and leucine zipper regions. The presence of GTP analog caused the quenching of the intrinsic fluorescence of the protein, suggesting interaction between the two molecules. The fluorescence gradually recovered as the nucleotide or its hydrolysis product dissociated from the protein.

GTP hydrolysis assays showed that EVC possessed a measurable intrinsic GTPase activity that obeyed Michaelis-Menten kinetics. The K_M , k_{cat}

and catalytic efficiency of the enzyme were calculated to be 0.820 mM, 0.175 sec⁻¹ and 213 M⁻¹sec⁻¹ respectively. Compared to other GTPases, the K_M was higher, indicating a low affinity of the protein for GTP. The leucine zipper caused the protein to form dimers could be seen on sodium dodecyl sulfate polyacrylamide gel electrophoresis (SDS-PAGE). In addition, the dimerization caused the protein to hydrolyze GTP to a mixture of GDP and GMP at unequal ratio. These kinetic parameters were similar to those displayed by large GTPases such as dynamin. It is proposed that the GTP-hydrolyzing activity of EVC protein is an important mechanistic step in the regulation of the hedgehog signaling pathways.

ACKNOWLEDGEMENTS

This work would not have been possible without the immense support of many individuals.

First, and foremost, I am deeply indebted to my thesis advisor, Dr. Oduyayo Odunuga for his support, guidance, encouragement and inspiration regardless of the place and time. Throughout the duration of this project, the door of his office was always open whenever I ran into a trouble spot or had a question about my research or writing. I truly appreciate all his invaluable advice, constructive criticism that were helpful for my thesis project and for my future career as well. He taught me a great deal about both scientific research and life in general and made my experience at SFA memorable.

I would like to express my deepest appreciation to all members of my thesis committee, Dr. Michele Harris, Dr. Matibur Zamadar, and Dr. Rebecca Parr for their kindly assistance, providing me with extensive personal as well as professional guidance. I am especially grateful to their patience and the precious time they spent reviewing my manuscript.

I cannot express enough thanks to the faculty and staff of the Department of Chemistry and Biochemistry at SFA. It is impossible for me to come this far without all of their help. I am grateful to Dr. Michael Janusa, Chair of the department for his belief in my work as well as in my abilities.

I could not have completed this project without the support and collaboration of my lab mate, Morgan Anderson. I very much appreciate all the moments we shared and the friendship created with her.

Finally, I am indebted to my beloved parents who always love, sacrifice and encourage me. My success would not have been possible without the support and nurturing of my parents. I give a sincere and heartfelt thank-you to them.

TABLE OF CONTENTS

ABSTRACT	i
ACKNOWLEDGEMENTS.....	iii
TABLE OF CONTENTS	v
LIST OF FIGURES	viii
LIST OF TABLES	x
CHAPTER 1	1
LITERATURE REVIEW	1
1.1 Ellis van Creveld syndrome	1
1.2 EVC protein	2
1.3 EVC2	6
1.4 EVC, EVC2 and the hedgehog signaling pathway	9
1.4.1 Hedgehog signaling pathway	9
1.4.2 Regulation of hedgehog signaling pathway by EVC proteins	10
1.4.3 EVC, hedgehog signaling pathway and cancer	14
1.5 Justification and hypothesis for study	14
CHAPTER 2	16
MATERIALS AND METHODS	16
2.1 Reagents and Materials.....	16
2.2 Plasmid constructs used for study	16
2.3 Transformation of competent <i>Escherichia. coli</i> BL21 (<i>DE3</i>)	17
2.4 Small-scale and time course expression analysis	18
2.5 Large-scale expression of EVC protein fragments in bacteria	18
2.6 Purification of EVC protein fragments using Ni-NTA agarose affinity column.....	19

2.7	Renaturation of partially purified denatured EVC protein fragments by gel filtration	20
2.8	Monitoring GTP binding to mEVC protein by fluorescence spectroscopy	21
2.9	Assay of putative guanosine triphosphatase (GTPase) activity of EVC protein	22
2.9.1	Optimization of EVC protein concentration for GTPase assay.....	23
2.9.2	Optimization of GTP concentration for GTPase assay	23
2.9.3	Time-course GTPase assay	23
2.9.4	EVC GTPase assay in the presence of pyrophosphatase	24
2.9.5	Bioinformatic analysis and modeling of EVC protein structures...	24
CHAPTER 3	25
RESULTS	25
3.1	Bioinformatic analysis.....	25
3.2	Mouse EVC and a mEVC2 protein fragments were successfully expressed in <i>E. coli</i> BL21 (<i>DE3</i>) cells.....	33
3.3	EVC protein fragments were successfully purified using Ni-NTA affinity combined with size exclusion chromatography.	34
3.3.1	Partial purification of hEVC and mEVC protein fragments was achieved by Ni-NTA affinity chromatography.....	34
3.3.2	Renaturation and simultaneous purification of denatured protein fragments by gel filtration.....	36
3.4	Monitoring GTP binding by intrinsic tryptophan fluorescence of mouse EVC proteins	37
3.5	Assay of the putative GTP hydrolyzing activities of EVC proteins	39
3.5.2	Time-course assay of GTPase activity of human EVC 546-661 ..	41
3.5.3	Optimizing concentration of mEVC 546-661 protein for GTPase assay	42
3.5.4	Mouse EVC GTPase activity at varying concentrations of GTP...	43
3.5.5	Hanes-Woolf plot for the GTPase activity of mEVC 546-661	44
CHAPTER 4	46

DISCUSSION	46
REFERENCES	56
APPENDIX A	63
APPENDIX B	64
VITA	65

LIST OF FIGURES

<u>Figure</u> 1. Domain and structural motifs in translated human EVC protein	3
<u>Figure</u> 2. Intrinsic tryptophan fluorescence of the wild-type and L298W hGBP-1 proteins	6
<u>Figure</u> 3. Mouse EVC2 protein	8
<u>Figure</u> 4. Mammalian hedgehog signaling pathway.....	10
<u>Figure</u> 5. Proposed model for EVC-EVC2 modulation of hedgehog signaling pathway.....	13
<u>Figure</u> 6. Domain organization of full-length mouse EVC protein	17
<u>Figure</u> 7. Chemical structure of (A) GTP analog GppNHp and (B) GTP	22
<u>Figure</u> 8. P-loop and Leucine zipper motifs in EVC sequences.....	25
<u>Figure</u> 9. Predicted 3D structure of mouse EVC protein using RaptorX	27
<u>Figure</u> 10. Predicted 3D - structure of human EVC protein using RaptorX.....	28
<u>Figure</u> 11. Arginine finger multiple sequence alignment.....	30
<u>Figure</u> 12. Predicted 3D structure of mouse EVC2 protein using RaptorX	31
<u>Figure</u> 13. Predicted 3D structure of human EVC2 protein by using RaptorX	32
<u>Figure</u> 14. SDS-PAGE showing expressed mEVC 546-661, mEVC 285-627, mEVC2 and hEVC 546-661 fragments	34
<u>Figure</u> 15. SDS-PAGE showing partially purified EVC and EVC2 protein fragments by Ni-NTA affinity chromatography	35

<u>Figure 16.</u> SDS-PAGE showing purified EVC proteins. (A) mEVC 546-661; (B) hEVC 546-661 and mEVC2; (C) mEVC 285-627	37
<u>Figure 17.</u> Intrinsic tryptophan fluorescence of mouse EVC protein fragments in the absence and presence of GTP analog GppNHp	38
<u>Figure 18.</u> Time – course assay of putative GTPase activity of mouse EVC	40
<u>Figure 19.</u> Reaction equation of m EVC 285-627 (A) and mEVC546-661(B)	40
<u>Figure 20.</u> Time – course assay of putative activity of human EVC	41
<u>Figure 21.</u> Optimal concentration of mEVC 546-661	42
<u>Figure 22.</u> Michaelis-Menten plot of the GTP hydrolyzing activity of mouse EVC protein	43
<u>Figure 23.</u> Hanes-Woolf plot of the GTPase activity of mEVC 546-661	45
<u>Figure 24.</u> Proposed model for the relationship between the structure and GTPase activity of EVC	55

LIST OF TABLES

Table 1. List of specialized reagents	16
Table 2. Plasmid constructs and their protein products	16
Table 3. Buffers used for Ni-NTA affinity purification	20
Table 4. Buffers used for gel filtration	21
Table 5. Kinetic parameters of mouse EVC GTP hydrolyzing activity	45

CHAPTER 1

LITERATURE REVIEW

1.1 Ellis van Creveld syndrome

The Ellis van Creveld (EvC) syndrome was first described by Richard W.B. Ellis of Edinburgh and Simon van Creveld of Amsterdam in 1940 (1). This syndrome is categorized as a rare autosomal recessive genetic abnormality. It is characterized by extra fingers or toes (polydactyly), short arms, legs, ribcage and stature (disproportionate dwarfism), and dysplasia nails. Dental abnormalities include short upper lip, multiple frenula, fusion or deficiency of teeth, mainly incisors (2).

In most parts of the world, the general population prevalence is 7 per 1,000,000 (3). However, the EvC syndrome is more common in the Amish population (Lancaster County, Pennsylvania, US) with significantly increased prevalence of 5 per 1000; so the frequency of carriers in this population may be as high as 13% (3). Sixty percent of patients affected by the syndrome have been reported with congenital cardiac defects; particularly defect in the atrial septation (3). EvC may be detected prenatally by ultrasound examination and the clinical diagnosis is based on observation of the manifestations of the symptoms described above. However, the definitive diagnosis is molecular analysis by direct sequencing for screening mutations in the *EVC* and *EVC2* genes (4).

Mutations in these two genes have been shown to be responsible for EvC syndrome (5). Clinical and molecular analyses reveal two novel heterozygous splice site mutations in intron 3 and intron 10 of the genomic *EVC* gene (5). These mutations caused the skipping of the entire exon 11 that possibly resulted in the absence of important functional domains in the protein (5). Altered splicing pattern in this mutation provided important insight in elucidating the pathogenesis of the EvC syndrome (5). Based upon data generated by the TCGA Research Network, 146 mutations in *EVC* and 278 mutations in *EVC2* have been reported in EvC patients including missense, nonsense, small frameshift insertions or deletions, splice site, in-frame deletions and large deletions mutations (6). A milder form of the syndrome is the Weyers acrofacial dysostosis (WAD) (4).

1.2 EVC protein

Polymeropoulos et al. (1996) mapped the gene for EvC syndrome to chromosome 4p16 (7). Ruiz-Perez et al. (2000) identified the *EVC* gene locus by positional cloning. The same authors (Ruiz-Perez et al., 2003) and others (Galdzicka et al., 2002) reported a second gene locus, *EVC2*, immediately adjacent to *EVC* in a head-to-head configuration (8-10). In human, the mRNA of *EVC* codes for a 112-kDa protein comprised of 992 amino acid residues. The primary sequence of EVC protein consists of several structural motifs including a P-loop motif, a leucine zipper, two putative nuclear localization signals, and a putative transmembrane domain (Figure 1) (11). EVC was shown to be present

at the base of non-motile cilia in cells (5). By *in situ* hybridization using whole mouse, EVC expression was observed in developing bones such as limbs, vertebrae and ribs (8).

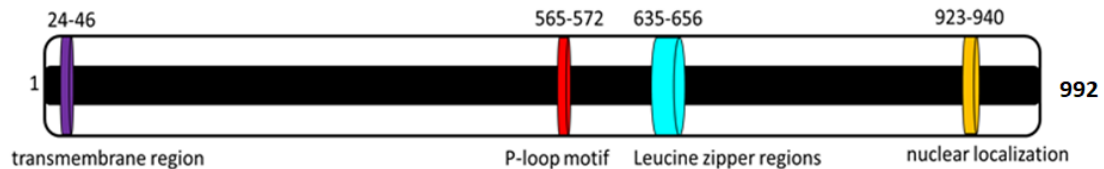


Figure 1. Domains and structural motifs in translated human EVC protein (11). Numbers represent positions of amino acid residues.

The P-loop or Walker (A) motif, is commonly found in ATP- and GTP-binding proteins and directly interacts with the phosphates of nucleotides (12,13). Typically, the P-loop has the consensus sequence G/AxxxxGK(S/T). The conserved lysine (K) residue of P-loop motif plays a crucial role in nucleotide-binding (12) by forming hydrogen bonds (H-bonds) with the β - and γ -phosphate groups of the NTP. From the other side, the serine (S) or threonine (T) residue binds between β - and γ -phosphates by coordinating the Mg^{2+} ion (14). All GTP-binding proteins require a Mg^{2+} ion for high affinity nucleotide binding because the negative charges of the phosphate groups are balanced by Mg^{2+} ion thus stabilizing the bound nucleotide (14). Ras is one of well-known small regulatory GTPases containing P-loop. It is reported that the Ras proteins, which are involved in the growth-promoting signal transduction pathways within the cell, possess a weak GTPase activity that is affected by mutations in the P-loop (15).

The presence of P-loop thus suggests that EVC possesses putative ATPase/GTPase activity.

The leucine zipper motif was first described as a dimerization domain in the yeast transcriptional factor GCN4, and in the oncogenic proteins Fos and Jun (16). Leucine zipper motifs are commonly found in proteins that regulate DNA transcription (transcription factors) (17). The leucine zipper motif is composed of two α helices, each containing a repetition of 4-5 leucines spaced seven residues apart, and kept together by hydrophobic interaction. Dimerization analysis by mutagenesis indicated that leucine residues of the leucine zipper motif are involved in the dimerization of RepA, a protein required for transcriptional autoregulation (16). The outcome of genetic and functional analysis of a leucine zipper-like motif located at the N-terminus of RepA revealed that leucine zipper motif modulates the equilibrium between monomeric and dimeric forms of the protein (16). In addition, residues in the motif have various functional roles, such as determining the specificity of heterodimerization, contributing moderately towards dimer stability, and determining the degree of oligomerization between the leucine zipper coiled-coils (16).

Previous studies have predicted that certain splicing errors readily occur just prior to a leucine zipper domain, which leads to suggestion that the putative leucine zipper domain may be important for protein function (5,11). However, the

biological function(s) of the putative leucine zipper motif found in EVC protein is still unknown.

A recent study reported that a hydrophobic α -helix present in human guanylate-binding proteins (hGBP1 and 2) is involved in the dimerization and regulation of the GTPase activities of the proteins (18). This α -helix is rich in hydrophobic residues such as isoleucine, leucine, and valine, making it structurally similar to a leucine zipper (18). This study suggested that binding of the nucleotide induces a conformational change in the wild-type hGBP-1 protein, which increases the total hydrophobicity upon exposure of the α -helix and thus mediates dimerization (18). Mutational disruption of this α -helix caused hGBP-1 to lose its ability to dimerize, and to hydrolyze GTP to GMP instead of GDP as shown by the wild-type protein (18)

The authors confirmed the importance of the hydrophobic helix for dimerization of hGBP-1 protein by monitoring the intrinsic tryptophan fluorescence of the protein in the presence and absence of the GTP analog, GppNHp (Figure 2). A mutant hGBP-1 containing an extra tryptophan engineered into the hydrophobic α -helix showed higher fluorescence than the wild type. However, the higher fluorescence of the mutant protein dropped drastically in the presence of GTP analog, while the wild type remained the same. These data confirmed that GTP binding to hGBP-1 caused hydrophobic residues in the α -helix to become exposed and thus resulted in dimerization of the protein.

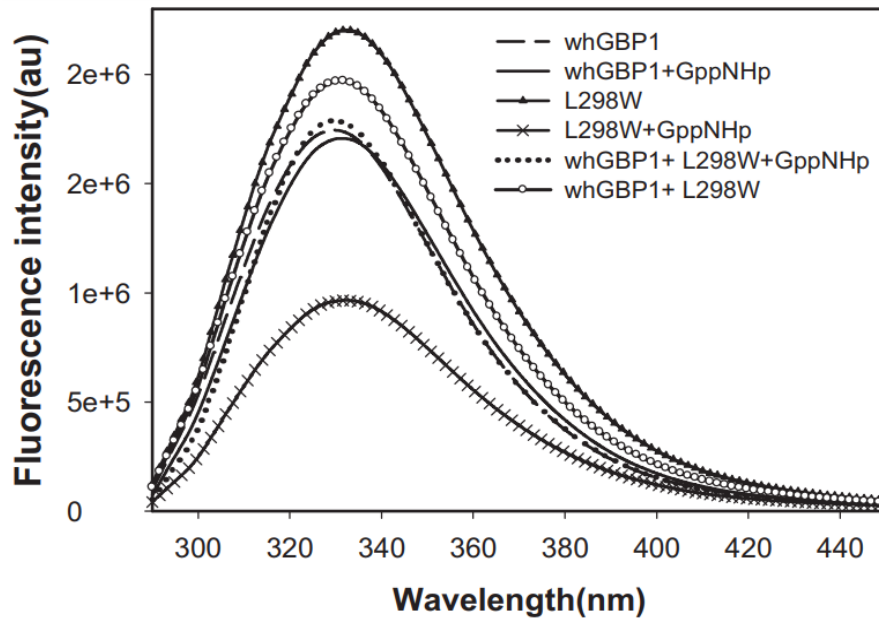


Figure 2. Intrinsic tryptophan fluorescence of the wild-type and L298W hGBP-1 proteins in the absence and presence of the substrate analog GppNHp (18).

1.3 EVC2

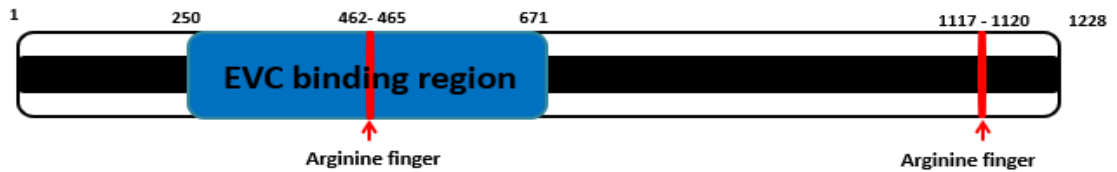
The Universal Protein Resource (UniProt) which provides sequences from annotated databases show that the genomic size of mouse *EVC2* gene is 166 kilobase pairs and its mRNA encodes a 1,228-amino acid protein that is approximately 139 kilodaltons (19). Mouse *EVC2* is in close proximity to *EVC* on the chromosome, and they are separated by 1,647 base pairs (9). It is suggested that *EVC* and *EVC2* act in a common pathway because of the indistinguishable phenotypes associated with mutations in either of the two genes (20). Based on their head-to-head configuration on the chromosome and proximity of their transcriptional start sites, it is suggested that coordinated expression of *EVC* and *EVC2* proteins is essential for maintaining their stoichiometric amounts in the cell

(20). By immunostaining analysis, EVC and EVC2 proteins were detected on the primary cilia in several different cell types and interestingly, the EVC2 protein was required for the localization of EVC protein at the base of primary cilia. Full-length mouse EVC2 protein was detected both in the cytoplasmic and in the nuclear fractions, but full-length mouse EVC protein was only detected in the cytoplasmic fractions by western blot analyses of mouse embryonic fibroblasts derived from null mice (20). To characterize the interaction between EVC and EVC2 proteins, deletion constructs of the genes were generated and used in a directed yeast-two-hybrid assay (20). Significant binding was observed between the mouse EVC2 fragment containing residues 250 – 671 and full-length mouse EVC. In addition, tagged EVC fragment (residues 463 – 1005) and EVC2 fragment (residues 250 – 671) co-precipitated from HEK 293 cells as confirmed by western blot analyses. These studies demonstrated that the two proteins physically interact in the cell.

Analysis of its primary structure revealed that mouse EVC2 contains two “arginine finger” motifs, (GxxR) (Figures 3A and B). One of the “arginine finger” motifs is located in the middle of the fragment (residues 250 – 671) that physically interacts with EVC (Figure 3A). The “arginine finger” is a motif that plays an important role in the mechanism of action of the GTPase activating proteins (GAPs). For example, the slow GTP hydrolysis by Ras is stimulated through interaction of its P-loop, switch I and switch II motifs with a GAP

containing an activating “arginine finger” that is highly conserved (21). The slow GTPase reaction rate of Ras is $4.7 \times 10^{-4} \text{ s}^{-1}$, but in the presence of GAP, the reaction rate increases to 19 s^{-1} at $25 \text{ }^\circ\text{C}$ (21). The “arginine finger” motif of GAP gets inserted into the active site of Ras, stabilizing the position of the catalytic glutamine 61 in switch II and neutralizing negative charges on the phosphates.

A



B

MGATGPTGAGGRATWVLAGNIIAAAALVLGSGPRALPPSFPALGPGSPSRPGPAGPWASSQYSDISREARG
 PFENGVIQKCSLVSGQSESQTMHVQLSVNNTTRPTSVNLSNLLVLDEITGLAVKESPGNNTQDGIQTFR
 KSFLQVGECYSVSYTASLDPTALGTGESLDLPARLIFQSPSQNRTQLKAPFTITVEEKIMVLPNHGLHAA
 GFMAAFLLISLLLTLAALFFLARGRCLQGGMLSRCRIQHPENKLEPSPFTSANGVSQDLSLNDQVVAIILTS
 EEPGSMQLQALEELEIATLNQADADLEACRNQISKDIIALLMKNLVSGGHLSPQTERKMAAAFKKQFLLLE
 NEIQEYERKMLALTAECDLEMRKKTENQYQREMVAMEEAEVLRKRVSESAECSLLRRTLHGLEQEDM
 QRSLLTLDQAEDFAQHRQLAVFQRNELHSIVYTIQISAVSK**GELR**PEVAKMMLQDYSKTQESVEELMDFD
 QATKRYHLSKRFGHREYLVQRLQAMETRVQGLLNTAATQLTSLIHKHERAGYLDEDQMETLLERAQTETF
 SIKQKLDNDLKQEKKRLHQRLITRRRRELLQKHKEQQKEQVSLGEASSTAEDAVQYLHQWRSVMAEHTAA
 LEELQERLDQAALDDLRLVLTVSLSEKATEELRRLQSTAMTQELLKRSAPWFLQQLIEEHSRESAARTTQ
 LEAEERERGGELVQGVQRRLQDDALEAYTEEQAELRHWEHLVFMKLCCAAISLSEEDLLRVRQEAQGCFS
 QLDRSLALPRVRARVLQQAQMAWREAEFRKLDQALAAPELQSKARKLRKGRGKADLLKKNLEDKIRLF
 EERAPVELADQVRGELLQERVQRLEAQEAHFAESLVALQFQVARAAETLSVYTALLSIQDLLLGELSES
 ETLTKSACVQIILESHRPELQELERKLEDQLVQEEAEQQRVLESWQRWAADGPGLEPEEMDPERQVSAI
 LRQALNKGQKLELQHQQRVREEWQNGAVLEDSLESIEADTMASLCSQGLRLVSYLSRMTMVPGSTLLRLL
 SVVLPAAASQPQLLALLDAVSEKHS DHTAENESSGEQAQAEQSKRRKHQVWVKVLD SRFADLV SQ**GLER**M
 LWARQKKERILKKIYVPVQERVMFPGKGSWPHLSLEPIGELAPI PITGADAMDILNTGEKIFVFRSPREP
 EISLRVPPRRKKNFLNAKKNRNLGLD

Figure 3. Mouse EVC2 protein. (A) Cartoon representation of EVC2 protein showing the fragment that binds to EVC (blue) and arginine finger motifs (red). Numbers represent positions of amino acid residues. (B) Sequence of mouse EVC2 protein showing positions of the “arginine finger” motifs (GxxR).

1.4 EVC, EVC2 and the hedgehog signaling pathway

1.4.1 Hedgehog signaling pathway

The hedgehog signaling (Hh) pathway ([Figure 4](#)) plays an important role in regulating cell growth and differentiation during normal human embryonic development (22). Key players in the hedgehog pathway in mammals include three ligands (Sonic, Indian and Desert), two receptors Patched (Ptch1, Ptch2), a signaling receptor smoothed (Smo) and three transcription factors (Gli1, Gli2, Gli3) (22). In the absence of the hedgehog ligand, the pathway is turned off by the twelve-pass transmembrane receptor Ptch, which inhibits the activation of Smo. Ptch suppresses Smo by maintaining it in a vesicle inside the cell. This leads to the inhibition of downstream cellular processes (22).

Hedgehog signaling is initiated when hedgehog ligands bind to Ptch receptor on the cell surface leading to internalization and degradation of Ptch. Removal of Ptch allows Smo to move from intracellular compartment to the cell surface where it initiates pathway. Smo accumulation in cilia ultimately leads to the transport of Gli and SuFu (Suppressor of Fused) complex to the tip of the cilium, allowing Gli to dissociate from SuFu and enter the nucleus to promote transcription of target genes (22).

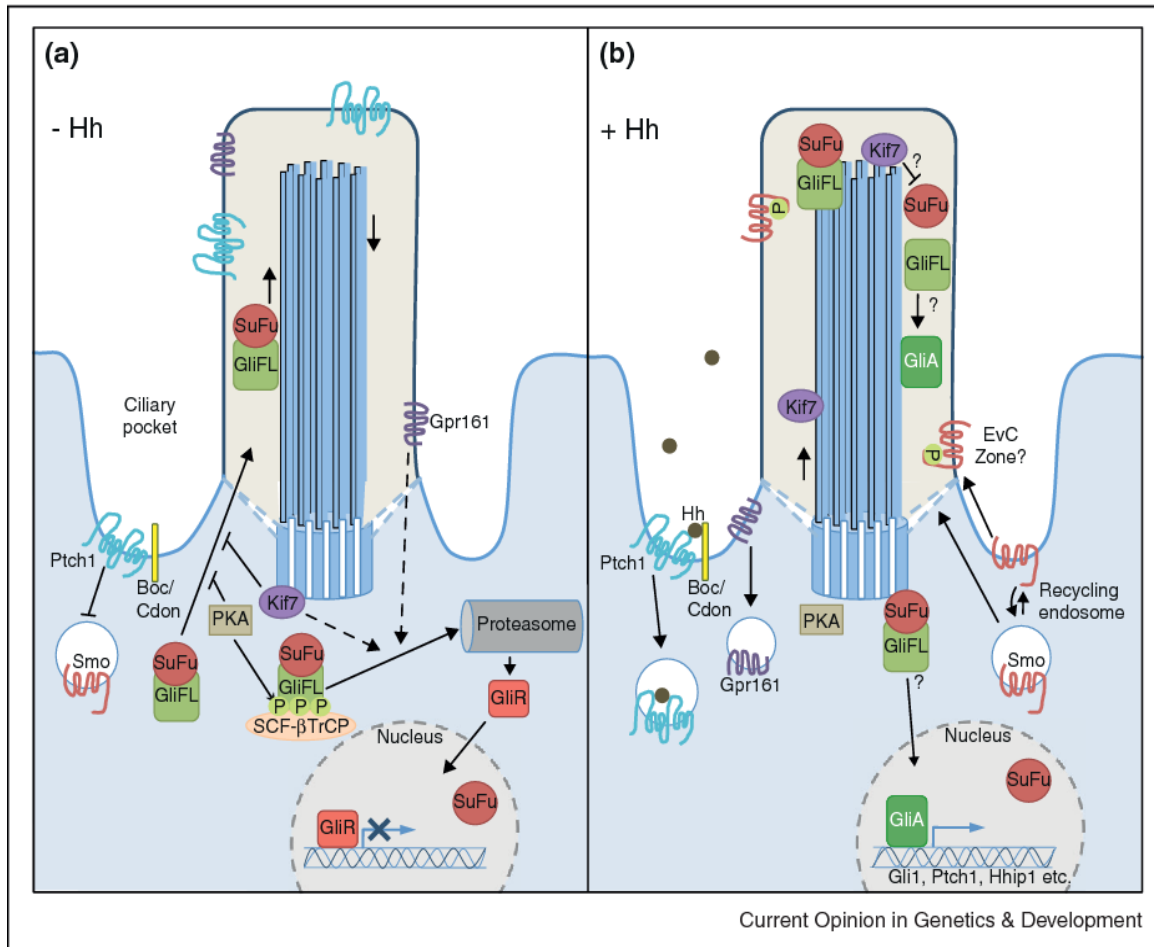


Figure 4. Mammalian hedgehog signaling pathway in the presence (A) and absence (B) of hedgehog ligands (23).

1.4.2 Regulation of hedgehog signaling pathway by EVC proteins

EVC and EVC2 proteins localize at the base of primary cilia in cells but are not essential for ciliogenesis (24). However, the proteins are positive regulators of the Hh signaling pathway, particularly the Indian hedgehog, resulting in transcription of target genes (24). EVC protein is present in normal developing skeleton and orofacial region (24). However, mice lacking the EVC

protein demonstrated skeletal and craniofacial abnormalities, but still survived to adult stages. Without the EVC protein, expressions of Ptch and Gli1 were significantly decreased, leading to diminished response to hedgehog signaling, but the Indian hedgehog signaling ligand was still expressed at normal level (24). It is known that Smo prevents phosphorylation and cleavage of full-length Gli3 to the transcriptional repressor Gli3R, and facilitates conversion of full-length Gli3 to the activator status, GliA. By western blot analysis, Gli3R was shown to be present in equal amounts in both EVC-depleted and normal mice. This observation implies that Gli3 proteolytic processing into Gli3R occurs normally even in mice lacking EVC. In addition, this observation suggests that EVC acts downstream of Smo to facilitate transcription of the Indian hedgehog target genes (24).

Knockdown of EVC2 expression in hedgehog reporter cells (LIGHT2) caused diminished response to purmorphamine, a Smo agonist (20). Similarly, Ptch1 expression in response to purmorphamine in EVC2 mutant mouse embryonic fibroblasts was reduced (20). This implies that EVC2 is a positive regulator of the hedgehog signaling pathway (20).

Based on emerging molecular and developmental studies, coordinated function of EVC and EVC2 proteins is required for cilia-dependent cardiac morphogenesis and related cellular processes (25). Although the mechanism by which EVC and EVC2 proteins cause identical phenotypes with characteristic

cardiac defects remains unknown, observations from co-localization studies in developing heart support the suggestion that the interaction of EVC and EVC2 proteins plays a role in atrioventricular structure development (25)

EVC and EVC2 proteins are ciliary proteins with predicted N-terminal transmembrane domains and regions of coiled-coil structure (Figure 5) (26). Endogenous EVC-EVC2 protein complexes were found at the primary cilia membrane and are required for normal endochondral growth and intramembranous ossification (26). It was revealed that EVC cooperated with EVC2 to maintain their normal protein levels and localization to primary cilia (26). This co-localization may explain why mutations in either gene results in the same phenotypes (26). EVC does not bind to EVC2 lacking the transmembrane region, however, this does not affect translocation of Smo to the cilium (26). This observation implies that the location of the EVC-EVC2 complex is critical for cellular response to hedgehog signaling (26). Loss of EVC2 has no effect on the cilia translocation of Smo, so by binding to Smo at the cilium base, EVC-EVC2 complexes promote hedgehog signaling (26).

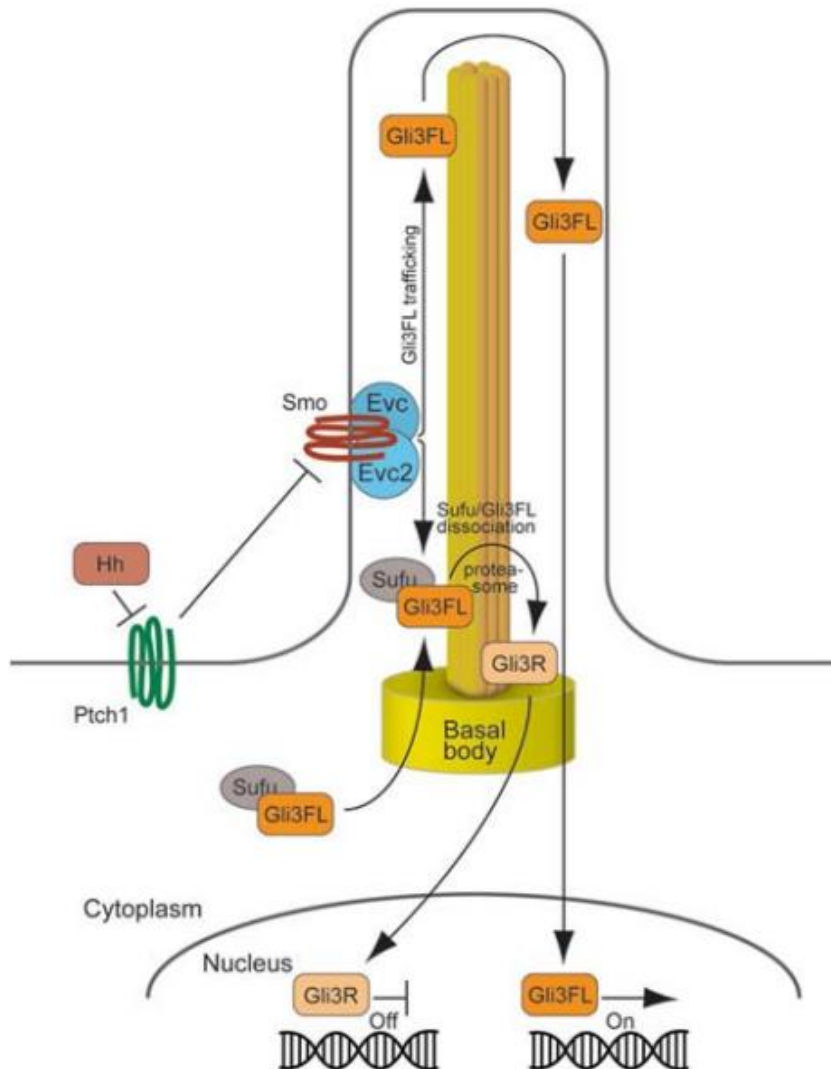


Figure 5. Proposed model for EVC-EVC2 modulation of hedgehog signaling pathway (26)

Furthermore, Gli3R levels were increased due to EVC2 deficiency (26). This indicates that lack of EVC2 results in impaired Sufu/Gli3FL dissociation and shifts the equilibrium of the Gli3R/Gli3FL ratio towards Gli3R. Also, cells lacking EVC2 show diminished movement of Gli3FL to the tip of cilium and less rapid accumulation of Gli3FL in the nucleus compared to normal cells. Furthermore,

overexpression of EVC and EVC2 equally disrupts the hedgehog signaling by decreasing level of Gli3FL and increasing the length of the cilium 1.51 times (26). As EVC-EVC2 complex is inhibited, the EVC-EVC2-Smo complexes display an abnormal distribution along the length of the cilium (26). This is another strong experimental evidence that shows that the location of the EVC-EVC2 complex in the cell is important in hedgehog signaling and that this location is at the base of the cilium where it interacts with Smo (26).

1.4.3 EVC, hedgehog signaling pathway and cancer

A recent study demonstrated that EVC protein was overexpressed in adult T-cell leukemia compared to normal cells, and that this overexpression increased the survival ability of the cells (27). Therefore, the authors implied that EVC could serve as a specific cell marker and a novel drug target for adult T-cell leukemia, and related cancers (27). Another study also showed that abnormal signaling in the hedgehog pathway may lead to cancer (28). These authors proposed that this abnormal signaling can occur through two different mechanisms: mutation-driven signaling and abnormal signaling in tumor environment (ligand-dependent signaling) (28). Thus, studying the role of EVC and EVC2 proteins in hedgehog signaling could define new targets for anti-cancer therapy.

1.5 Justification and hypothesis for study

EVC and EVC2 proteins play crucial roles in hedgehog signaling pathway during cardiac development and pathogenesis of EvC syndrome (3). However,

the functions and mechanisms of action of these proteins in hedgehog signaling are not fully understood. The *EVC* gene encodes a protein with putative P-loop and leucine-zipper motifs, suggesting its putative ability to bind and hydrolyze nucleotides, as well as dimerize. This study would be the first attempt to test the potential GTP-binding and hydrolyzing activities of EVC protein experimentally. The outcome of the project would provide important mechanistic information about the role EVC in the regulation of the hedgehog signaling pathway. The study was divided into the following objectives:

1. Express and purify EVC proteins to homogeneity
2. Assay for the putative nucleotide-binding and hydrolyzing activities of EVC protein.
3. Characterize the effect of EVC2 on the putative nucleotide-binding and hydrolyzing activities of EVC protein.

CHAPTER 2

MATERIALS AND METHODS

2.1 Reagents and Materials

Table1: List of Specialized Reagents

Reagent	Cat #	Company
CytoPhosphate kit	BK054	Cytoskeleton Inc.
GTP	G8877	Sigma
GTP analog GppNHp	G0635	Sigma
Pyrophosphatase	9024-82-2	Sigma

2.2 Plasmid constructs used for study

DNA sequences coding for fragments ([Figure 6](#)) of mouse EVC (mEVC) protein were previously cloned into the pET28a bacterial expression vector to generate various mEVC plasmid constructs (Table 2). Dr. Odunuga provided these constructs for this study.

Table 2: Mouse EVC plasmid constructs and their protein products

Name of constructs	Size of gene (bp)	Protein size (kDa)	Structural motif(s) present
pET28a His-mEVC 546-661	348	15.4	P-loop and Leucine zipper
pET28a His-mEVC 286-627	1029	40.1	P-loop
pET28a His-hEVC 546-661	348	15.5	P-loop and Leucine zipper
pET28a His-mEVC2	945	39.3	Arginine finger

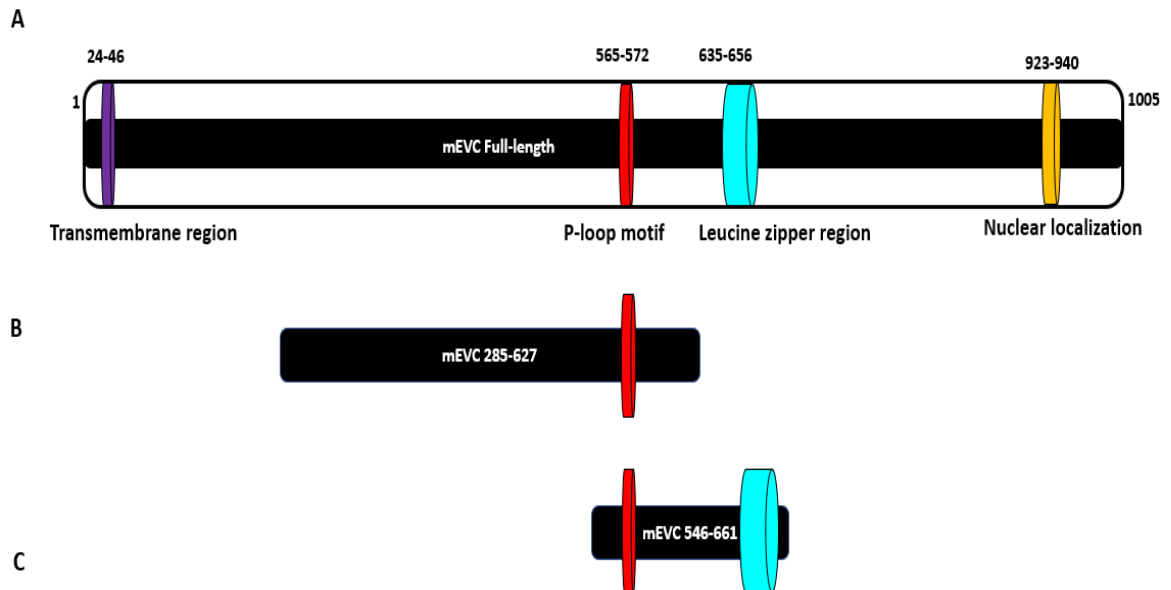


Figure 6. Domain organization of full-length mouse EVC protein and its fragments used for study (A) Cartoon showing the domain structure of full-length mouse EVC protein with transmembrane, P-loop motif, leucine zipper region, and nuclear localization signals depicted as cylinders, (B) fragment mEVC 285-627 containing only P-loop motif, (C) fragment mEVC 546-661 containing both P-loop and leucine zipper motifs

2.3 Transformation of competent *Escherichia coli* BL21 (DE3)

The plasmid constructs were used to transform competent *Escherichia coli* BL21 (DE3) cells for expression. 50 μ L of the cells were thawed on ice before adding 1 μ L of 100 ng/ μ L plasmid DNA. The mixture was kept on ice for 20 minutes and then heat-shocked at 42 °C for 40 seconds. After that, the cells were incubated on ice for 2 additional minutes before adding warm LB broth to a 1-mL final volume. The mixture was incubated at 37 °C with shaking at 250 rpm for 30 minutes. 100 μ L of the culture was spread onto a LB agar plate containing 50 μ g/mL kanamycin and incubated overnight at 37 °C.

2.4 Small-scale and time course expression analysis

Single colonies from LB agar-kanamycin plates were randomly picked and transferred to culture tubes containing 5 mL of LB broth with 50 µg/mL kanamycin, and incubated overnight at 37 °C, with shaking at 250 rpm. 250 µL of the overnight culture was used to inoculate a fresh 25 mL of LB broth containing 50 µg/mL kanamycin. The cultures were grown at 37 °C with constant shaking at 250 rpm until an optical density (OD) reading at 600 nm showed an absorbance of approximately 0.6 to 0.9. Protein expression was induced by adding 400 µM isopropyl β-D-1-thiogalactopyranoside (IPTG). At one-hour increment, over a total of 5 hours, 1-mL sample of the culture was aliquoted. The expression of EVC protein fragments was analyzed on 15% sodium dodecyl sulfate polyacrylamide gel electrophoresis (SDS-PAGE).

2.5 Large-scale expression of EVC protein fragments in bacteria

After transforming *E. coli* BL21 (*DE3*) with plasmid constructs, single colonies were used to inoculate 25 mL of LB broth containing 50 µg/mL of kanamycin. The cultures were grown overnight at 37 °C with constant shaking at 250 rpm and then the overnight culture was used as stock culture for large-scale expression. Fresh 1 Liter LB broth containing the 50 µg/mL of kanamycin was inoculated to a ratio of 1: 200. Cultures were grown at 37 °C until they reached an OD at 600nm of 0.6 (approximately 3 to 4 hours) before adding 400 µM IPTG to induce protein expression. The inoculated cultures were allowed to incubate for 4

hours at 37 °C with constant shaking. A 1-mL aliquot was collected before and after induction with IPTG, pelleted and analyzed for the expression of EVC protein fragments using 15% SDS-PAGE. Cells were harvested by centrifuging at 6,000 × *g* for 15 minutes at 4 °C, and the supernatant was discarded. The cells were lysed immediately or stored at -80 °C for future use.

2.6 Purification of EVC protein fragments using Ni-NTA agarose affinity column

Purification of EVC protein fragments was carried out using a combination of denaturing and native buffers (Table 3). Induced bacterial cell pellets that had expressed EVC protein fragments were resuspended in 1:20 to 1:10 culture volume of native buffer (Table 3) containing DNase (40 unit/L of culture), lysozyme (3 mg/L of culture) and PMSF (1 mM final). The mixtures were gently stirred at room temperature for 15 minutes before they were mechanically lysed in a French press. The lysates were incubated at room temperature for 15 minutes before adding 9 M urea denaturing buffer to make a final concentration of 8 M urea buffer. After mixing well for 15 minutes at room temperature, the lysates were centrifuged at 15,000 × *g* for 45 minutes at 4 °C. Then, the supernatants were filtered using Buchner funnel with 0.45 µm filter paper to remove particulate matter. After equilibrating Ni-NTA column with 8 M urea denaturing buffer, the supernatants were loaded onto the column at a flow rate of 1 mL/min. The columns were washed first with 8 M urea denaturing buffer at pH

8.0 followed by the same buffer at pH 6.3. Proteins were eluted with 10 X resin volume of 8 M urea denaturing buffer at pH 4.5. Eluted proteins were analyzed on 15% SDS-PAGE.

Table 3. Buffers used for Ni-NTA affinity purification

Buffer	Reagents
Native buffer	100 mM NaH ₂ PO ₄ , 10 mM Tris, pH 8.0
Stock denaturing buffer	9 M urea, 100 mM NaH ₂ PO ₄ , 10 mM Tris, pH 8.0
Normal denaturing buffer	8 M urea, 100 mM NaH ₂ PO ₄ , 10 mM Tris, pH 8.0
Wash buffer	8 M urea, 100 mM NaH ₂ PO ₄ , 10 mM Tris, pH 6.3
Elution buffer	8 M urea, 100 mM NaH ₂ PO ₄ , 10 mM Tris, pH 4.5

2.7 Renaturation of partially purified denatured EVC protein fragments by gel filtration

Denatured partially purified EVC proteins from Ni-NTA affinity column were subjected to reverse-gradient gel filtration on a Superdex 200 preparative grade column to refold the proteins and simultaneously remove contaminants and phosphate from the mixture (29). Gradient gel filtration was performed in several cycles until the proteins were completely or nearly refolded. In the first cycle, concentrated partially purified denatured proteins were loaded onto the gel filtration column that was equilibrated with buffer A (Table 4). Elution was carried out with a reverse urea gradient of 6 M to 0 M (buffer A to buffer B, Table 4) at a flow rate of 0.5 to 1 mL/min.

Generally, EVC proteins were eluted between 3 M and 4 M urea. Eluted EVC protein was concentrated and loaded onto the column containing 3 M to 4 M urea

for a second gel filtration cycle. Elution was repeated as above with urea gradient of 3 or 4 M to 0 M urea. If necessary, a third gel filtration cycle was performed. Otherwise, eluted protein was concentrated using Amicon centrifugal filters (Millipore Sigma). The purity of refolded EVC proteins was analyzed on 15% SDS-PAGE.

Table 4. Buffers used for gel filtration

Buffer	Reagents
Buffer A	0 M urea, 50 mM Tris, 200 mM NaCl, 1 mM DTT, pH 7.5
Buffer B	6 M urea, 50 mM Tris, 200 mM NaCl, 1 mM DTT, pH 7.5

Protein concentration was determined using the Bradford colorimetric assay. 10 μ L of protein sample was diluted to 1 mL in ddH₂O. 1 mL of ready-to-use Bradford reagent (Thermo Scientific) was added and the mixture allowed to incubate at room temperature for 10 minutes before absorbance was read at 595 nm. A linear standard graph (see Appendix A) was generated using varying concentrations of bovine serum albumin (BSA) to extrapolate absorbance value into μ g protein solution and used to determine the concentration of EVC protein fragments.

2.8 Monitoring GTP binding to mEVC protein by fluorescence spectroscopy

The intrinsic fluorescence of mEVC protein fragments was measured in the absence and presence of the GTP analog, GppNHp ([Figure 7A](#)) in a Perkin Elmer LS-55 spectrometer. Reaction buffer containing 50 mM Tris, pH 7.5, 1 mM

MgCl₂ and 4 μM of mEVC protein was incubated at room temperature for 10 minutes. The reaction was started by adding 0.5 mM GppNHp to a final reaction volume of 500 μL. The tryptophan fluorescence emission spectra were measured by exciting the sample at 280 nm and collecting the emitted fluorescence at 290 nm and 450 nm.

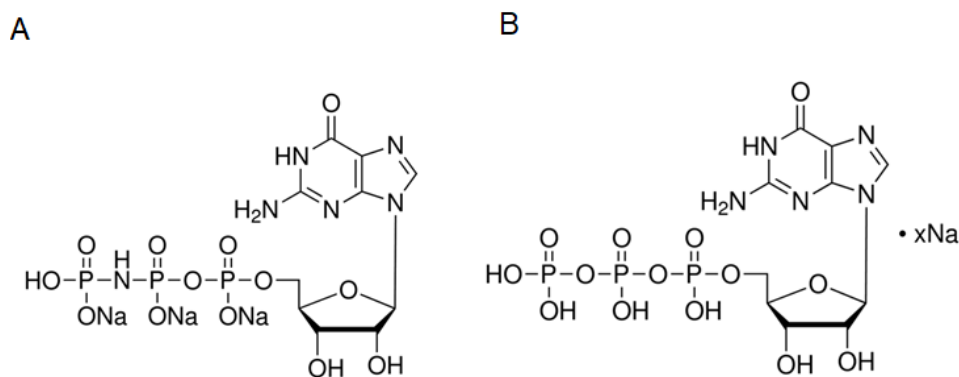


Figure 7. Chemical structure of (A) GTP analog GppNHp and (B) GTP

2.9 Assay of putative guanosine triphosphatase (GTPase) activity of EVC protein

Previous study revealed that EVC does not hydrolyze ATP [30]. Therefore, EVC proteins were tested for their ability to hydrolyze GTP (Figure 7B), using the Cytophosphate kit from Cytoskeleton Incorporation. Briefly, assay was performed in a 300-μL reaction mixture containing 50 mM Tris, pH 7.5, and 1 mM MgCl₂. Purified EVC proteins were incubated in the assay buffer at 37 °C for 10 minutes before adding GTP to start the reaction. Inorganic phosphate formed after specific reaction time was measured colorimetrically at 650 nm by adding a

malachite-green dye mixture that simultaneously quenched the reaction. Activity was measured as the inorganic phosphate released per unit time. All assays were performed at least in duplicates.

2.9.1 Optimization of EVC protein concentration for GTPase assay

GTPase activity was assayed using 1 mM of GTP in 300 μ L total volume of assay buffer with varying concentrations of mEVC protein fragments as follows: 0.250 μ M, 0.500 μ M, 0.750 μ M, 1.00 μ M, 1.25 μ M, 1.50 μ M, 1.75 μ M, 2.00 μ M. The amount of inorganic phosphate (Pi) in the reaction mixture was determined by extrapolation from a standard Pi graph. By subtracting Pi released from GTP autolysis, the actual amount of Pi released by EVC-dependent GTP hydrolysis in reaction mixture was calculated. The concentration of mEVC protein releasing the highest amount of Pi was used in subsequent assays.

2.9.2 Optimization of GTP concentration for GTPase assay

The assays were repeated as described above using 2 μ M mEVC protein and varying concentrations of GTP as follows: 0.100 mM, 0.250 mM, 0.500 mM, 1.00 mM, 1.50 mM, 2.00 mM, 2.50 mM, 3.00 mM. Optimal concentrations of mEVC and GTP, 2 μ M and 2 mM respectively, were used in subsequent assays.

2.9.3 Time-course GTPase assay

GTPase activity was assayed using 2 μ M mEVC protein and, 2 mM GTP in 300 μ L total volume of assay buffer. The reactions were stopped at the

following time points: 0.50 min, 1.0 min, 1.5 min, 2.0 min, 3.0 min, 4.0 and 5.0 min.

2.9.4 EVC GTPase assay in the presence of pyrophosphatase

Having established optimal assay conditions as 2 μ M mEVC, 2 mM GTP and 3 min incubation time, GTPase assays were repeated with and without addition of 1U of pyrophosphatase. EVC protein and pyrophosphatase were incubated together in assay buffer at 37 °C before adding GTP to start the reaction. 1U of pyrophosphatase was established as excess based on manufacturer's protocols.

2.9.5 Bioinformatic analysis and modeling of EVC protein structures

EVC protein sequences of various animals were obtained from NCBI and then multiple sequence alignment of these sequences was carried out using Clustal Omega (31). Three-dimensional structure of hEVC, mEVC, mEVC2 and hEVC2 proteins were modeled by using RaptorX – a protein structure prediction webserver which is hosted at the University of Chicago (32-36) and then visualized by Chimera (37).

CHAPTER 3

RESULTS

3.1 Bioinformatic analysis

Multiple sequence alignment of EVC protein sequences from various animals was carried out using Clustal Omega (31). Data obtained revealed the presence of the P-loop motif in EVC sequences. The P-loop motif of primate origin (Figure 8A) was found to be highly conserved as the consensus sequence, AxxxxGKS.

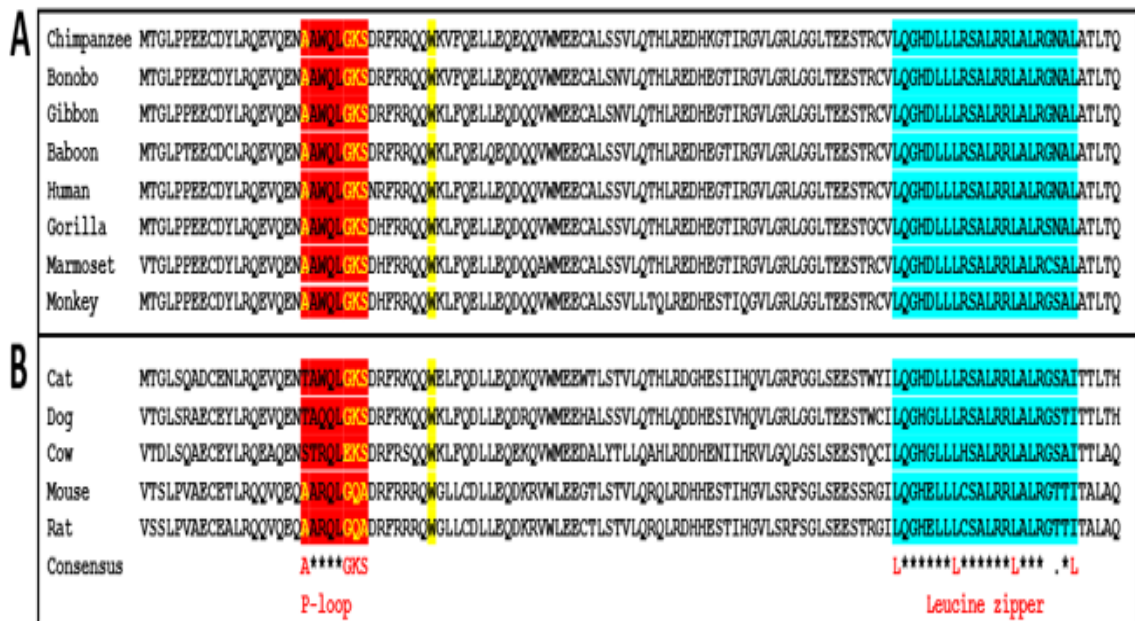


Figure 8. P-loop and Leucine zipper motifs in EVC sequences
 (A) The P-loop and leucine zipper motifs in EVC sequences of primate origin are highly conserved, (B) The P-loop and leucine zipper motifs in the sequences of other animals are less conserved.

However, the P-loop motif found in EVC sequences of other species are less conserved (Figure 8B). For example, instead of the real P-loop residues (AxxxxGKS) found in human EVC (hEVC), the mouse EVC (mEVC) contains the residues AxxxxGQA (Figure 8B). This sequence lacks the conserved lysine (K), which has been shown to be important for nucleotide-binding (12). In addition, the P-loop motif in mEVC sequence contains a terminal alanine instead of the canonical serine (S) or threonine (T) residue, which coordinates with the Mg^{2+} ion that binds with the β - and γ -phosphates of nucleotides (14). Primate EVC sequences also have conserved leucine zipper containing the consensus sequence LxxxxxxLxxxxxxLxxxxxxL (Figure 8A). However, multiple sequence alignment showed that other species such as cat, dog, cow, mouse and rat consist of less-conserved leucine zipper motifs with a terminal isoleucine instead of leucine (Figure 8B).

Using RaptorX – a protein structure prediction webserver that is hosted at the University of Chicago (32-36) – the three-dimensional structures of hEVC, mEVC, mEVC2 and hEVC2 proteins were modeled and then visualized by Chimera (37). The predicted structures of mouse and human EVC proteins revealed that P-loop is exposed, thus ensuring access to solvated GTP (Figures 9A and B, and 10A and B).

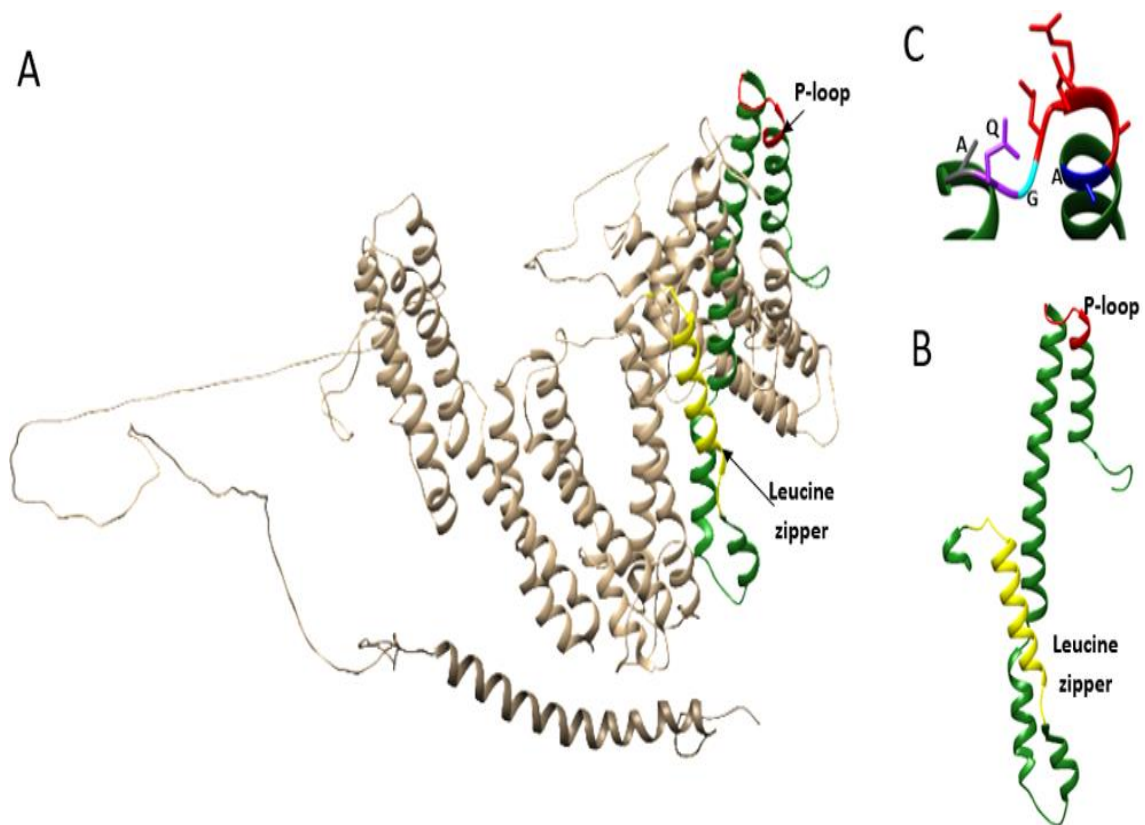


Figure 9. Predicted 3D structure of mouse EVC protein using RaptorX (A) Full-length mouse EVC, (B) mouse EVC fragment 546-661 containing potential P-loop (red) and leucine zipper motifs (yellow), (C) P-loop (AxxxxGQA) residues (32-36) Molecular graphics and analyses were performed with UCSF Chimera, developed by the Resource for Biocomputing, Visualization, and Informatics at the University of California, San Francisco, with support from NIH P41-GM103311.

One of the important residues in the P-loop of hEVC sequence is a lysine residue ([Figure 10C](#)) whose side chain has been implicated in hydrogen bonding to the γ -phosphate of nucleotides (12). The amine group ($-\text{NH}_3^+$) group of lysine residue also contributes to neutralizing negative charges on the phosphate groups (38). Following the lysine in the P-loop of hEVC, the serine also provides an oxygen atom ([Figure 10C](#)) that coordinates with the divalent cation associated with the bound nucleotide (14). Instead of lysine - a basic, charged amino acid,

mEVC has glutamine (Figure 9C) which is classified as a charge-neutral, polar amino acid. Glutamine contains an amide group in its side chain; therefore, it has electron pairs available for hydrogen bonding to water and other molecules. The carbonyl group can function as a hydrogen bond acceptor, and the amino group (NH₂) can function as a hydrogen bond donor. In addition, serine - a polar uncharged amino acid is also substituted by alanine- a nonpolar amino acid that does not possess an oxygen atom in its side chain.

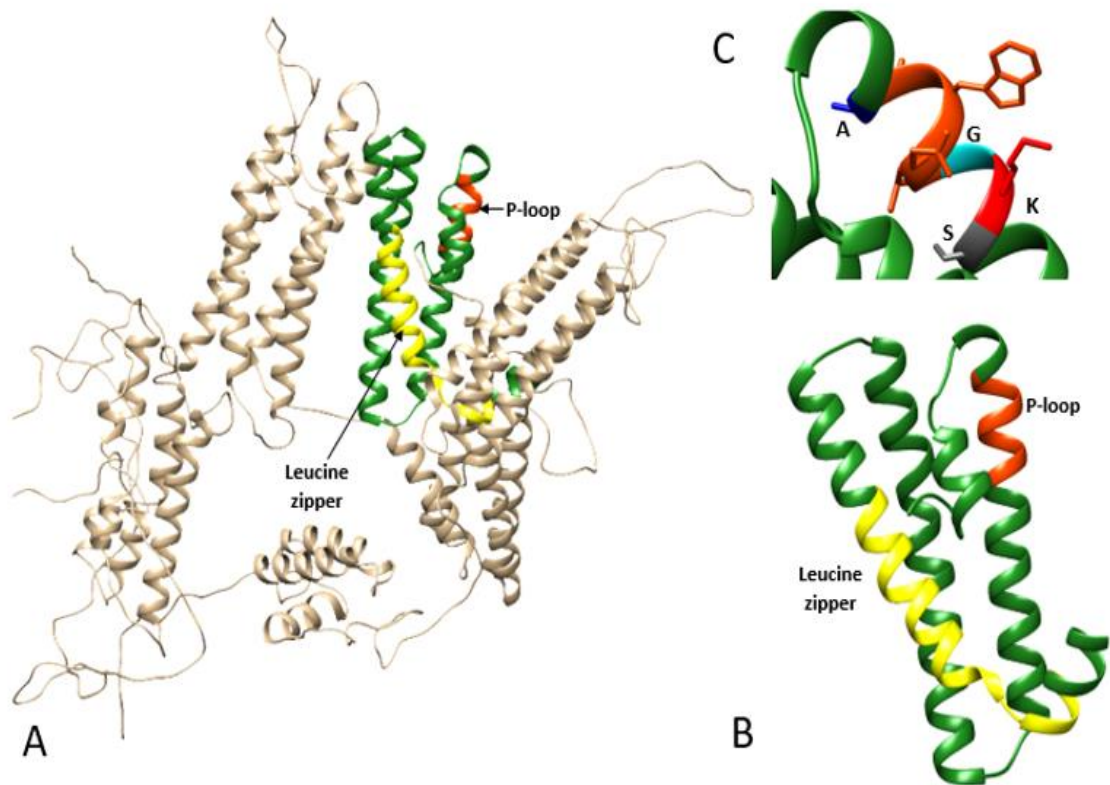


Figure 10. Predicted 3D - structure of human EVC protein using RaptorX (A) Full-length human EVC, (B) human EVC fragment 546-661 containing P-loop (red) and leucine zipper motifs (yellow), (C) P-loop (AxxxxxGKS) residues (32, 36) Molecular graphics and analyses were performed with UCSF Chimera, developed by the Resource for Biocomputing, Visualization, and Informatics at the University of California, San Francisco, with support from NIH P41-GM103311.

The predicted structures of mouse and human EVC proteins (Figures 9A and 10A) show that the leucine zipper is sufficiently exposed to potentially allow the interaction of two EVC molecules at that position so that dimerization can occur. Furthermore, the leucine zipper is opposite the P-loop (Figures 9B and 10B) which ensures that the protein can bind and hydrolyze GTP in its dimeric form.

GTPase activity of Ras is activated through interaction of its active site with the “arginine finger” of another protein called GTPase activating protein (GAP) (21). The “arginine finger” motif (GxxR) is conserved in GAPs (21). Therefore, multiple sequence alignment of EVC2 protein sequences was screened for the presence of arginine fingers (Figure 11).

It was discovered that mEVC2 consists of two arginine fingers - GELR (residues 461-464) and GELR (residues 1116-1119). The first arginine finger is located in the EVC-binding region (residues 250-671) of mEVC2. The human, gorilla and chimpanzee sequences (all primates) have three arginine fingers: GEER, GRRR and GKLR.

Baboon	HRIFFTQIKSAILKGLKPEAAKTLNQNSKIQENVEELMDFQASKRYHLSKRFHGHEY	497
Gorilla	RSIFFTQIKSAIFKGLKPEAAKMLLNQNSKIQENVEELMDFQASKRYHLSKRFHGHEY	517
Chimpanzee	HSIFFTQIKSAIFKGLKPEAAKTLNQNSKIQENVEELMDFQASKRYHLSKRFHGHEY	597
Human	HSIFFTQIKSAIFKGLKPEAAKMLLNQNSKIQENVEELMDFQASKRYHLSKRFHGHEY	597
Hamster	RSIVYTQIQSAVAKGELRPEVAKMLLDQYSKTQERVEELMDFQATKRYHLSKRFHGHEY	507
Mouse	HSIVYTQIQSAVSKGELRPEVAKMLLDQYSKTQESVEELMDFQATKRYHLSKRFHGHEY	507
Rat	HSIVYTQIQSAVAKGELRPEVAKMLLDQYSKTQESIEELMDFQATKRYHLSKRFHGHEY	507
	:*.:***:**:****:*.**:*:**:*** ** :*****:*****	
Baboon	EEHGKEMAVRAEQLEGEERDRDQEGVQSVRQRLKDDAPEAATEEQAELRRWEHLVFMKLC	737
Gorilla	EEHGKEMAARAQLEGEERDRDQEGVQSVRQRLKDDAPEAVTEEQAELRRWEHLVFMKLC	757
Chimpanzee	EEHGKEMAARAQLEGEERDRDQEGVQSVRQRLKDDAPEAVTEEQAELRRWEHLVFMKLS	837
Human	EEHGKEMAARAQLEGEERDRDQEGVQSVRQRLKDDAPEAVTEEQAELRRWEHLVFMKLC	837
Hamster	EEHSRESAARTAQLEAEEREHGQELVQGVRRQLQQDLPEACTEEQAELRHWEHLVFTKLC	747
Mouse	EEHSRESAARTTQLEAEERERGGQELVQGVRRQLQQDALEAYTEEQAELRRWEHLVFMKLC	747
Rat	EEHSRESAARTAQLEAEERERGGQELVQGVRRQLQQDAPEACTEEQAELRHWEHLVFTKLC	747
	:.*.*::***:..** ** :*****:* ** *****:****:* **.	
Baboon	DSKLRGDLISRGLEKMLWARKRKQSVLKKSCPLRERMIFSGKGSWPHLSLEPIGELAPV	1155
Gorilla	DGKLRGDLISRGLEKMLWARKRKQSVLKKCTCLPLRERMIFSGKGSWPHLSLEPIGELAPV	1175
Chimpanzee	DGKLRGDLISRGLEKMLWARKRKQSVLKKCTCLPLRERMIFSGKGSWPHLSLEPIGELAPV	1255
Human	DGKLRGDLISRGLEKMLWARKRKQSVLKKCTCLPLRERMIFSGKGSWPHLSLEPIGELAPV	1255
Hamster	DSRLRADLVSGGLERMLWAHQKESILKKVYTPVQERVTFPGKGSWPHLSLEPIGELAPI	1162
Mouse	DSRFADLVSGGLERMLWARRKKEERILKKIYVPVQERVVFPKGGSWPHLSLEPIGELAPI	1164
Rat	DSRFADLVSGGLERMLWARRKKEESILKKRYVPVQERVVFPKGGSWPHLSLEPIGELAPI	1164
	.:.*:**:***:*****:..: :*** ** :*** * *****	
Baboon	TLRRLSVVLPPTASQPQLLALLDSGSRHPDHAEEGDG--GAEQADVGRRRKHQSWMQAF	1095
Gorilla	TLRRLSVVLPPTASQPQLLALLDSATERHADHAAESDG--GVEQVDVGRRRKHQSWMQAL	1115
Chimpanzee	TLRRLSVVLPPTASQPQLLALLDSATERHADHAAESDG--GAEQADVGRRRKHQSWMQAL	1195
Human	TLRRLSVVLPPTASQPQLLALLDSATERHVDHAAESDG--GAEQADVGRRRKHQSWMQAL	1195
Hamster	TLRRLSVVLPVAVASQPQLLALLDVTSEKHSOHTAENGSSGDP--AEQEKBBKHQSWMQAL	1102
Mouse	TLLRRLSVVLPAAASQPQLLALLDAVSEKHSOHTAENESSGGEQAQAEQSKRRKHQVWVKVL	1104
Rat	TLLRRLSVVLPAAASQPQLLALLDAVSEKHSOHTAENESSGGEQAQAEQSKBBKHQSWMKAL	1104
	** *****:*****: :*.* ** :*. . :. :.***** **.:	
Baboon	DSKLRGDLISRGLEKMLWARKRKQSVLKKSCPLRERMIFSGKGSWPHLSLEPIGELAPV	1155
Gorilla	DGKLRGDLISRGLEKMLWARKRKQSVLKKCTCLPLRERMIFSGKGSWPHLSLEPIGELAPV	1175
Chimpanzee	DGKLRGDLISRGLEKMLWARKRKQSVLKKCTCLPLRERMIFSGKGSWPHLSLEPIGELAPV	1255
Human	DGKLRGDLISRGLEKMLWARKRKQSVLKKCTCLPLRERMIFSGKGSWPHLSLEPIGELAPV	1255
Hamster	DSRLRADLVSGGLERMLWAHQKESILKKVYTPVQERVTFPGKGSWPHLSLEPIGELAPI	1162
Mouse	DSRFADLVSGGLERMLWARRKKEERILKKIYVPVQERVVFPKGGSWPHLSLEPIGELAPI	1164
Rat	DSRFADLVSGGLERMLWARRKKEESILKKRYVPVQERVVFPKGGSWPHLSLEPIGELAPI	1164
	.:.*:**:***:*****:..: :*** ** :*** * *****	

Figure 11. Arginine finger motifs in EVC2 sequences from various animal

The three-dimensional structures of human and mouse EVC2 were also modelled using RaptorX server (32, 36) and visualized by Chimera. The predicted structure of mouse EVC2 (Figure 12A) shows that the fragment binding EVC (blue) (Figure 12B) contains the first arginine finger (GELR, residues 461-464). This arginine finger is in the EVC-binding region of mEVC2 and locates on

the surface of mEVC2 suggesting that it may play a significant role in the interaction between mEVC2 and mEVC. The arginine residue - a basic amino acid containing a guanidino group in side chain - is adjacent to the glycine residue (Figure 12C) making a closed structure of arginine finger motif. However, the second arginine finger (GLER, residues 1116-1119), which is in a non EVC-binding region is hidden inside the protein structure. This implies that this second arginine finger may not be involved in interaction of mEVC2 with mEVC protein.

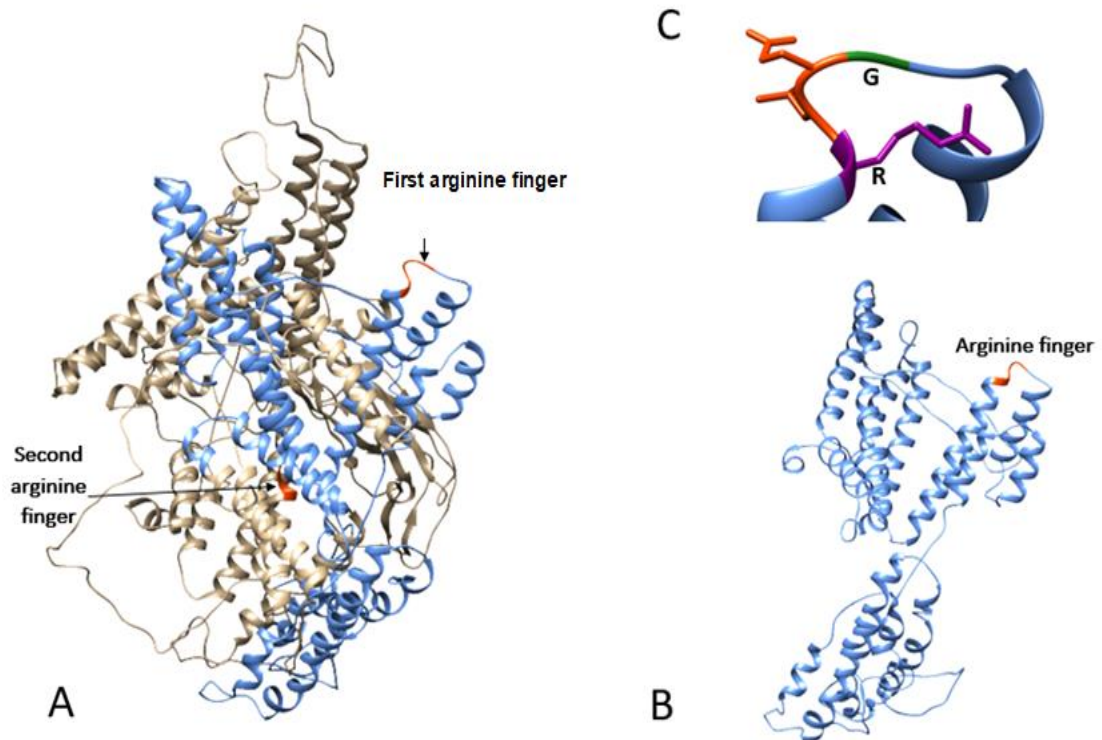


Figure 12. Predicted 3D structure of mouse EVC2 protein using RaptorX (A) Full-length mouse EVC2 protein containing EVC binding region (hot pink) and two arginine finger motifs (yellow), (B) EVC binding region, (C) Arginine finger (GxxR) in EVC binding region (32, 36)

Molecular graphics and analyses were performed with UCSF Chimera, developed by the Resource for Biocomputing, Visualization, and Informatics at the University of California, San Francisco, with support from NIH P41-GM103311

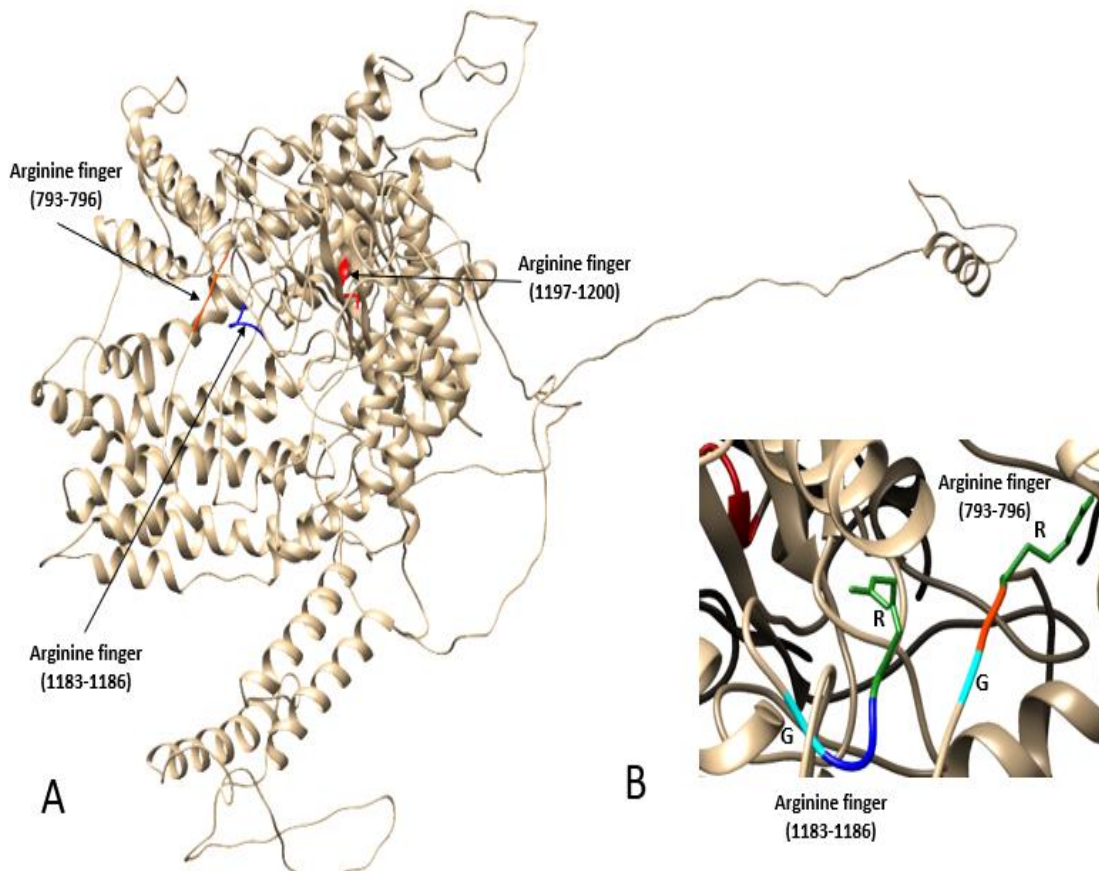


Figure 13. Predicted 3D structure of human EVC2 protein by using RaptorX
 (A) Full-length human EVC2 protein containing three arginine finger motifs (orange, blue and red),
 (B) First and second arginine fingers (GxxR) in close proximity (32, 36)
 Molecular graphics and analyses were performed with UCSF Chimera, developed by the Resource for Biocomputing, Visualization, and Informatics at the University of California, San Francisco, with support from NIH P41-GM103311

Unexpectedly, hEVC2 has three putative arginine fingers that do not locate at the surface of the protein (Figure 13A). However, the first (residues 793-796) and the second (residues 1183-1186) arginine fingers are still somewhat exposed to the surrounding environment, but not completely like mEVC2. Although they are separated by 390 amino acids, they are close to each other in the protein structure, and there is no barrier between them (Figure 13B).

Interestingly, the glycine residue of the first finger is close and opposite to the arginine of the second finger. This indicates that both may cooperate and have a role in the interaction with hEVC protein. The third finger (1197-1200) is completely hidden inside the hEVC2 and therefore it may not be involved in interaction with hEVC.

3.2 Mouse EVC and a mEVC2 protein fragments were successfully expressed in *E. coli* BL21 (DE3) cells

Expression of different mouse EVC and EVC2 protein fragments was induced by 0.4 mM IPTG at 37 °C with shaking at 250 rpm. Samples of expression cultures were collected at 1 hour (t_1), 3 hours (t_3) and 5 hours (t_5). Whole bacterial lysates containing expressed mEVC and mEVC2 proteins were analyzed on SDS-PAGE ([Figure 14](#)).

The mEVC 546-661 ([Figure 14A](#)), mEVC 286-627 ([Figure 14B](#)), mEVC2 ([Figure 14C](#)) and hEVC 546-661 ([Figure 14D](#)) fragments were successfully expressed in bacteria as confirmed by the protein bands running at the expected mobilities of 15.4 kDa, 41.5 kDa, 39.3 kDa and 15.5 kDa respectively. The time-course analysis indicated that the expression of the proteins occurred stably after 5 hr. post induction, however the expression levels between 3 hr. and 5 hr. post induction was not significantly different. Therefore, the subsequent large-scale expression was carried at 37 °C for 3 hr. post induction.

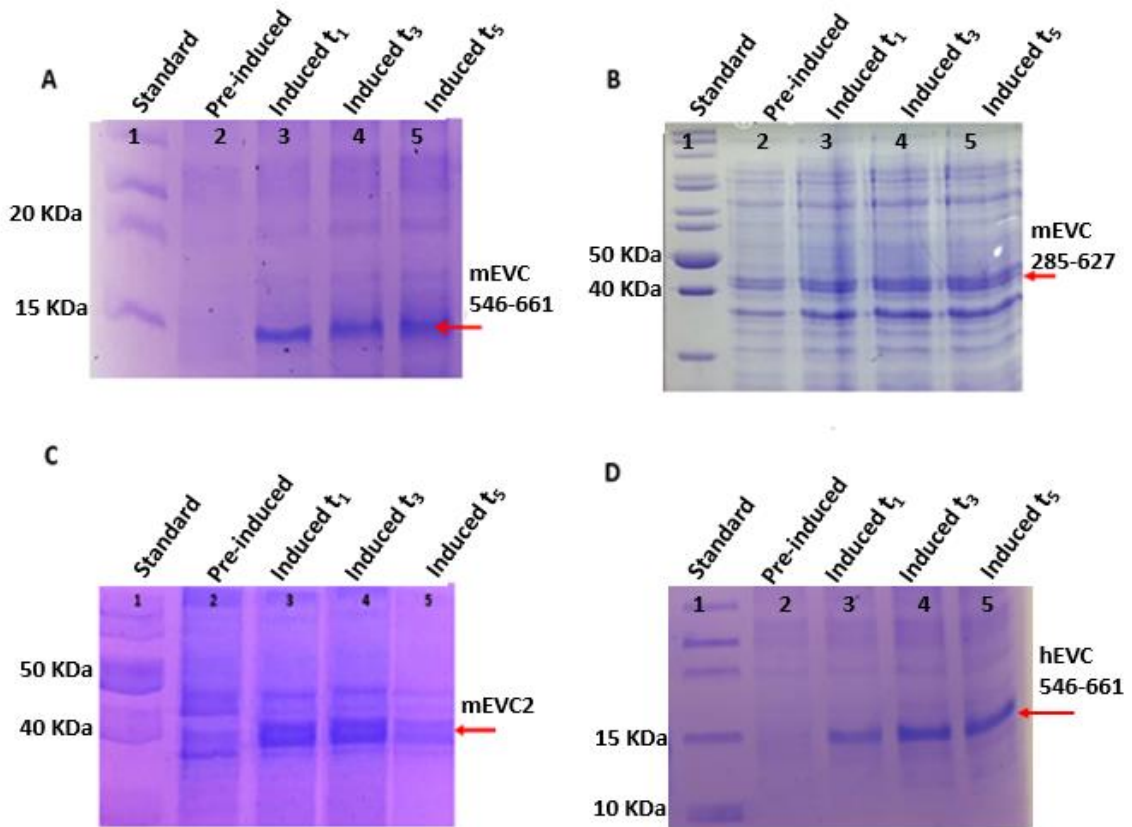


Figure 14. SDS-PAGE showing expressed mEVC 546-661 (A), mEVC 285-627(B), mEVC2 (C) and hEVC 546-661 (D) fragments

3.3 EVC protein fragments were successfully purified using Ni-NTA affinity combined with size exclusion chromatography.

3.3.1 Partial purification of hEVC and mEVC protein fragments was achieved by Ni-NTA affinity chromatography

Human and mouse EVC protein fragments were found in the insoluble portion (pellet) of bacterial cell lysates when cells were lysed in native buffer.

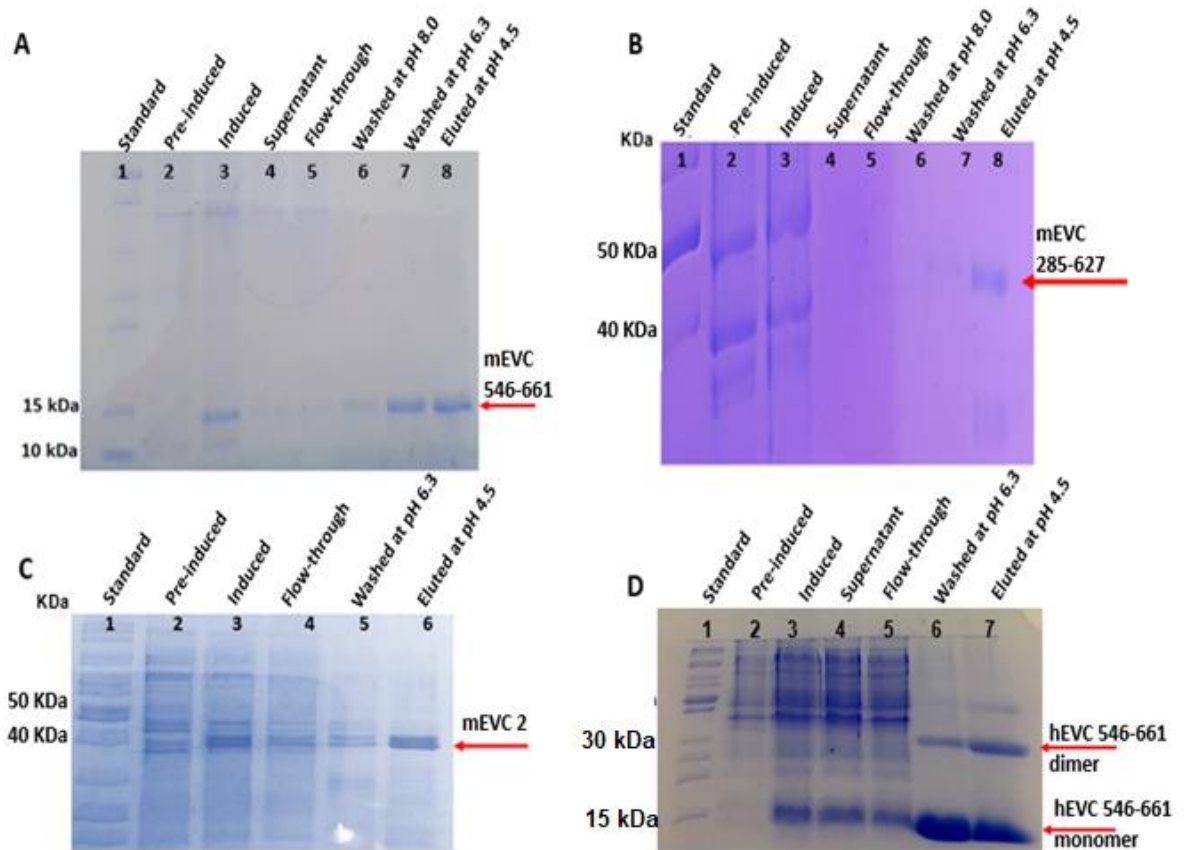


Figure 15. SDS-PAGE showing partially purified EVC and EVC2 protein fragments by Ni-NTA affinity chromatography (A) mEVC 456-661, (B) mEVC 285-627, (C) mEVC2, (D) hEVC 546-661

The presence of 8 M urea denatured the proteins and then shifted the solubility of the denatured proteins from pellet to supernatant. After centrifuging the lysate, the supernatant was loaded onto the column and proteins were eluted with denaturing buffer at pH 4.5. Ni-NTA affinity chromatography yielded EVC and EVC2 proteins that were relatively pure (Figures 15, A to D)

3.3.2 Renaturation and simultaneous purification of denatured protein fragments by gel filtration

The purpose of performing gel filtration was to obtain higher level of purify, refold the proteins, and remove phosphate from the buffer. Proteins were eluted from gel filtration column by performing a decreasing urea gradient from 6 M to 0 M. Gel filtration was repeated starting at previous urea concentration until proteins were deemed refolded. Reloaded proteins were thereafter concentrated. The reverse gradient approach prevented precipitation of the protein during refolding.

SDS-PAGE analysis for mEVC 546-661 and hEVC 546-661 showed extra protein bands at about 27 kDa size which is the size of dimeric form of the proteins (Figures 16A and B). mEVC 546-661 and hEVC 546-661 fragments consist of a leucine zipper which was first described as a dimerization domain in the yeast transcriptional factor GCN4 and in the oncogenic proteins Fos and Jun (16). Therefore, it implies that dimeric form of mEVC 546-661 fragment was formed via the leucine zipper motif. SDS-PAGE analysis of mEVC 285-627 and mEVC2 proteins showed that gel filtration equally yielded high level of purity (Figures 16B and C).

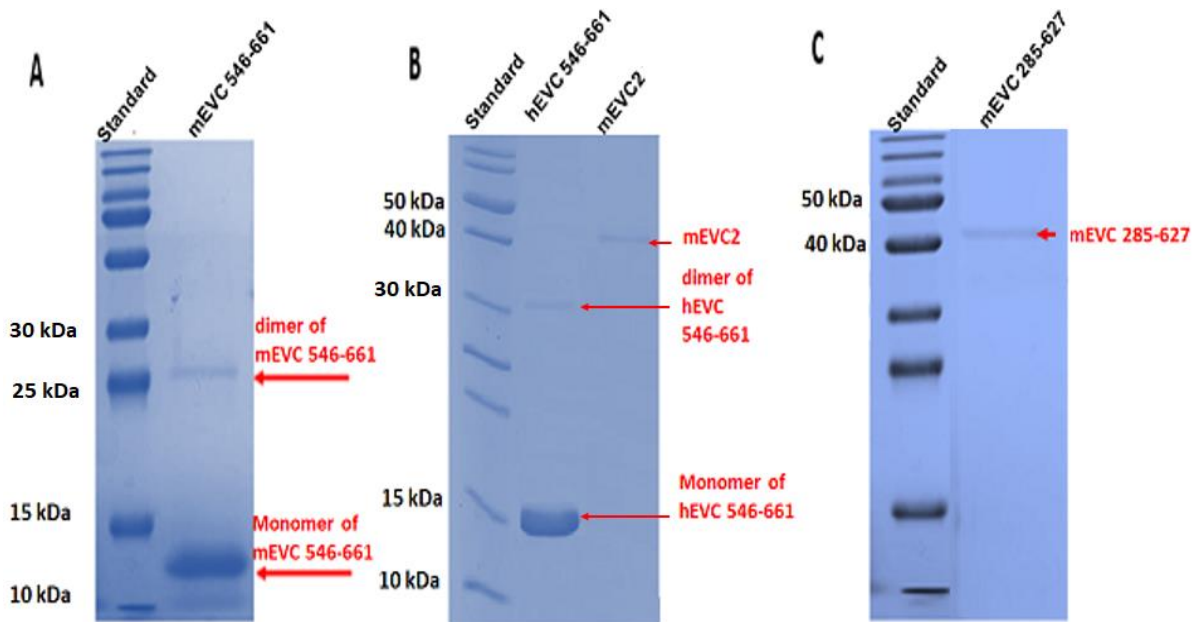


Figure 16. SDS-PAGE showing purified EVC proteins

(A) mEVC 546-661, (B) hEVC 546-661 and mEVC2, (C) mEVC 285-627

3.4 Monitoring GTP binding by intrinsic tryptophan fluorescence of mouse EVC proteins

Intrinsic protein fluorescence is mainly due to tryptophan. As the local environment surrounding the indole ring changes due to the protein conformational transitions, subunit association, ligand binding or denaturation, the emission spectrum of tryptophan is affected and changes. In this study, tryptophan fluorescence emission spectra were measured by exciting the sample at 280 nm and collecting the emitted fluorescence from 290 and 450 nm.

In the absence of GTP analog GppNHp, fragment mEVC 285-627 produced highest fluorescence intensity of about 600 au (Figure 17A). However,

the fluorescence intensity was quenched drastically to about 180 au after 30 seconds of adding the analog. The intensity decreased further to about 100 au after 2 minutes. However, there was a slight increase in intensity after 10 minutes of adding the GTP analog.

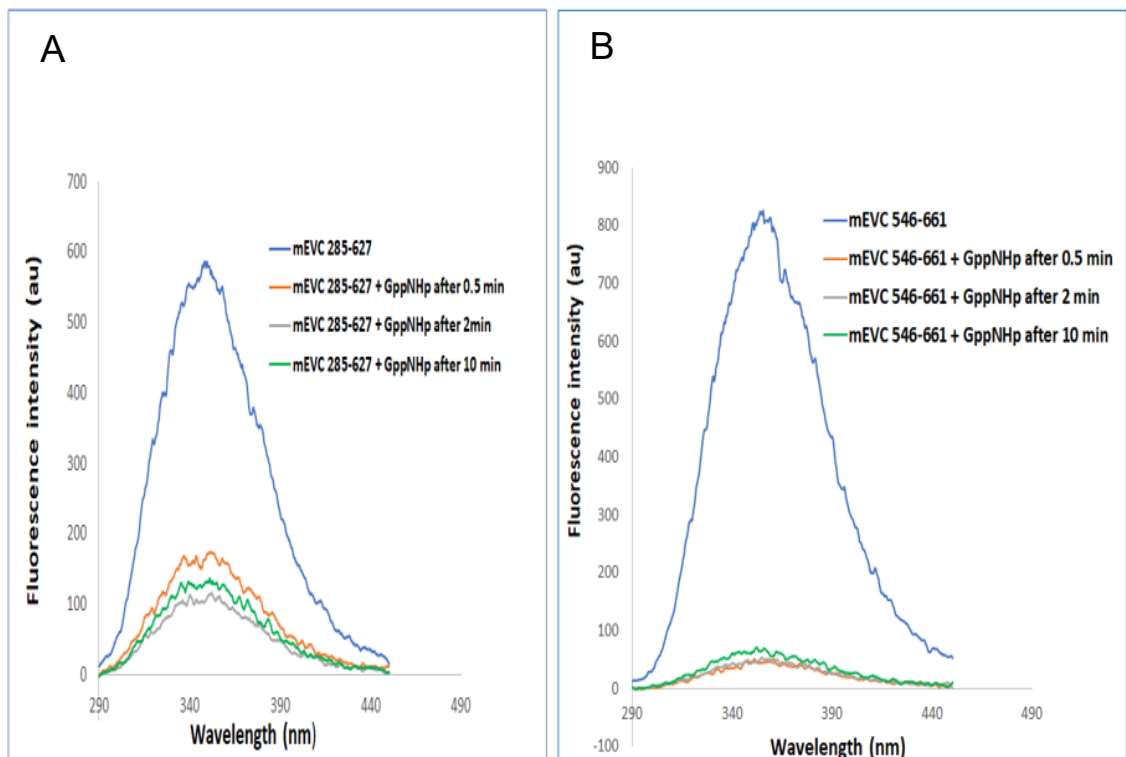


Figure 17. Intrinsic tryptophan fluorescence of mouse EVC 285-627 (A) and EVC 546-661 (B) in the absence and presence of GTP analog GppNHp. The concentration of the enzyme was kept at 4 μ M, and 0.5 mM analog was used for the assay. The samples were excited at 280 nm and the fluorescence emission spectra were recorded between 290 and 450 nm.

In the absence of the GTP analog GppNHp, fragment mEVC 546-661 produced highest fluorescence intensity of about 800 au (Figure 17B). However, the fluorescence intensity was drastically quenched to about 50 au after 30 seconds

of adding the analog. The intensity remained the same after 2 minutes. However, there was a slight increase in intensity to about 70 au after 10 minutes.

The result suggested that both fragments mEVC 285-627 and mEVC 546-661 were able to bind to GTP. The fragment mEVC 285-546 containing P-loop appeared to bind the analog at a slower rate than the fragment mEVC 546-661, which contains both P-loop and leucine zipper motifs.

3.5 Assay of the putative GTP hydrolyzing activities of EVC proteins

3.5.1 Time-course assay of GTPase activity of mEVC 285-627 and mEVC 546-661

Time-course GTP hydrolysis assay was carried out in the absence and presence of pyrophosphatase enzyme that hydrolyzes P₂i to P_i ([Figure 18](#)). The assay using mEVC 285-627, which contains P-loop only, showed no trace of inorganic phosphate (P_i). However, the presence of P_i was revealed after pyrophosphatase enzyme was added to the reaction ([Figure 18A](#)). This implies that mEVC 285-627 released P₂i, the substrate for pyrophosphatase enzyme, instead of P_i ([Figure 19A](#)). Assay of the fragment mEVC 546-661, containing P-loop and leucine zipper motifs, released P_i even without pyrophosphatase enzyme. However, the amount of P_i increased in the presence of pyrophosphatase ([Figure 18B](#)). This data indicates that the fragment mEVC 546-661 hydrolyzes GTP to a mixture of GDP + P_i and GMP + P₂i ([Figure 19B](#)).

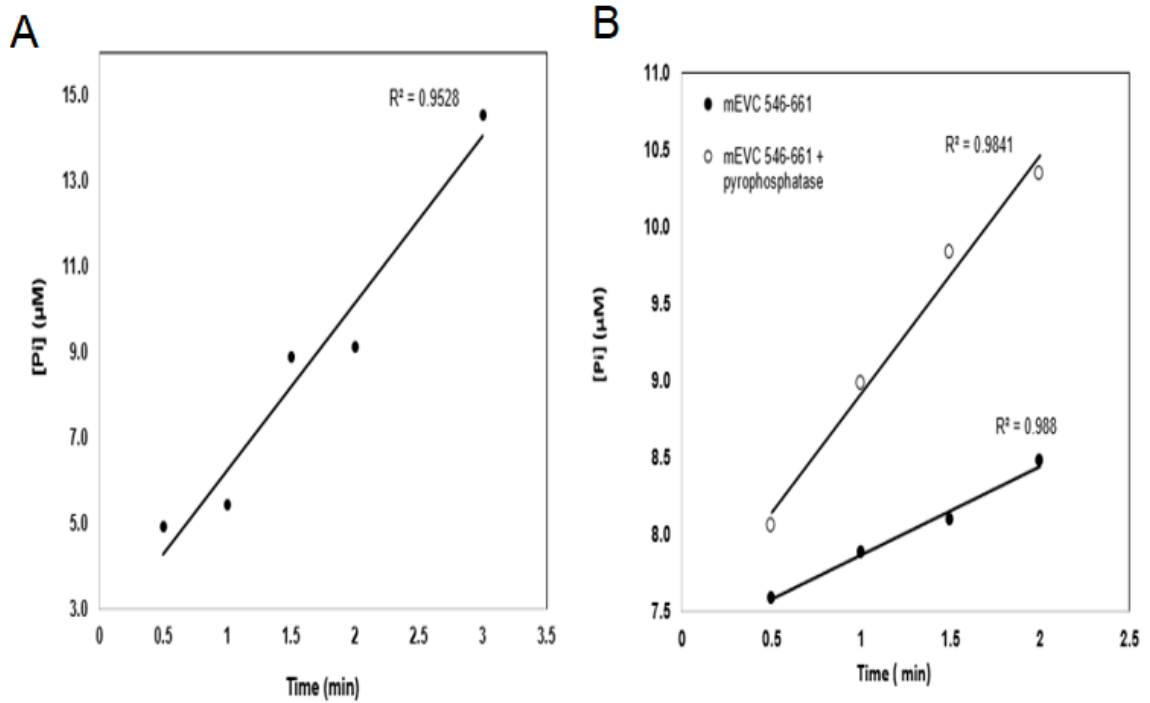


Figure 18. Time – course assay of putative GTPase activity of mouse EVC
 (A) Time-course GTPase assay of mouse EVC 285-627 fragment. (B) Time-course GTPase assay of mouse EVC 546-661 fragment
 GTPase activity was assayed using 2 μM of either mouse EVC 546-661 (A) or EVC 285-627 (B) protein in 300 μL total volume of buffer containing 50 mM Tris, pH 7.5, 1mM MgCl₂, 2 mM GTP with or without 1 U of pyrophosphatase. Inorganic phosphate released was measured colorimetrically using a malachite-green dye assay at 650 nm. All assays were performed at least in duplicates.

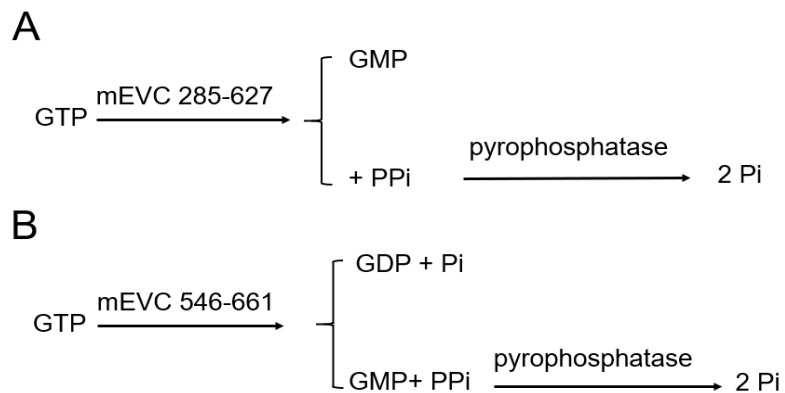


Figure 19. Reaction equations of mEVC 285-627 (A) and mEVC546-661(B)

3.5.2 Time-course assay of GTPase activity of human EVC 546-661

The human EVC 546-661 fragment, which also consists of P-loop and leucine zipper motif, showed a GTP hydrolysis activity that was higher than that of mEVC, both in the presence and absence of pyrophosphatase (Figure 20). This result also indicates that the fragment hEVC 546-661 hydrolyzes GTP to a mixture of GDP + Pi and GMP + PPI. Interestingly, only 20 nM hEVC 546-661 was used for the assay compared with 2 μ M mEVC (100 times more).

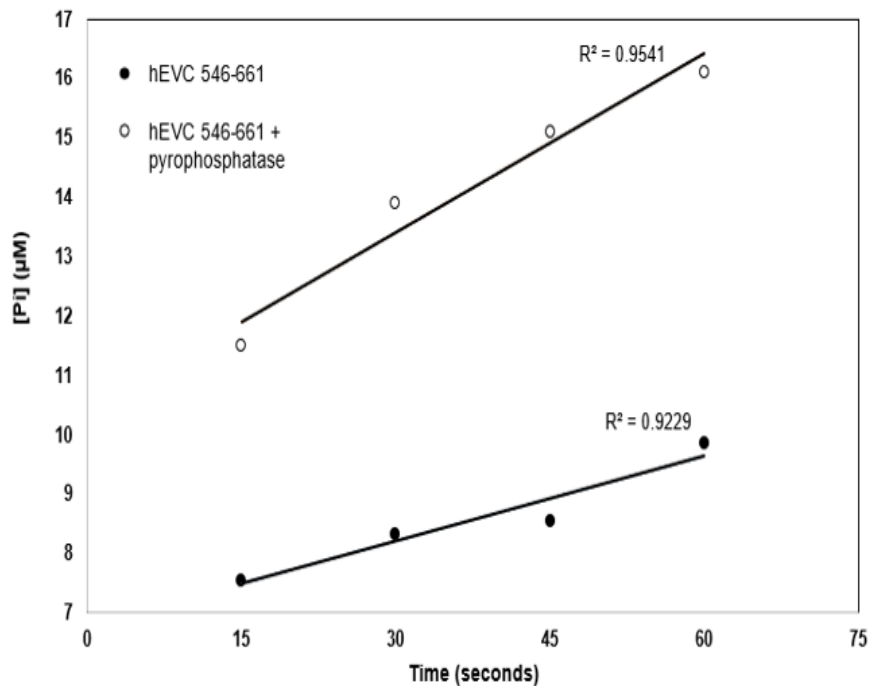


Figure 20. Time-course assay of putative activity of human EVC GTPase activity was assayed using 20 nM of hEVC 546-661 in 300 μ L total volume of buffer containing 50 mM Tris, pH 7.5, 1 mM $MgCl_2$, 2 mM GTP with or without 1 U of pyrophosphatase. Inorganic phosphate released was measured colorimetrically using a malachite-green dye assay at 650 nm. All assays were performed at least in duplicates.

3.5.3 Optimizing concentration of mEVC 546-661 protein for GTPase assay

The concentration of mEVC 546-661 giving the highest Pi released was determined by varying concentrations of enzyme as follows: 0.250 μM , 0.500 μM , 0.750 μM , 1.00 μM , 1.25 μM , 1.50 μM , 1.75 μM , and 2.00 μM (Figure 21).

GTPase activity was assayed using 1 mM of GTP in 300 μL total volume of assay buffer. Figure 21 shows that 2 μM of mEVC 546-661 gave highest Pi releasing (10.34 μM) and this concentration was used in subsequent experiments.

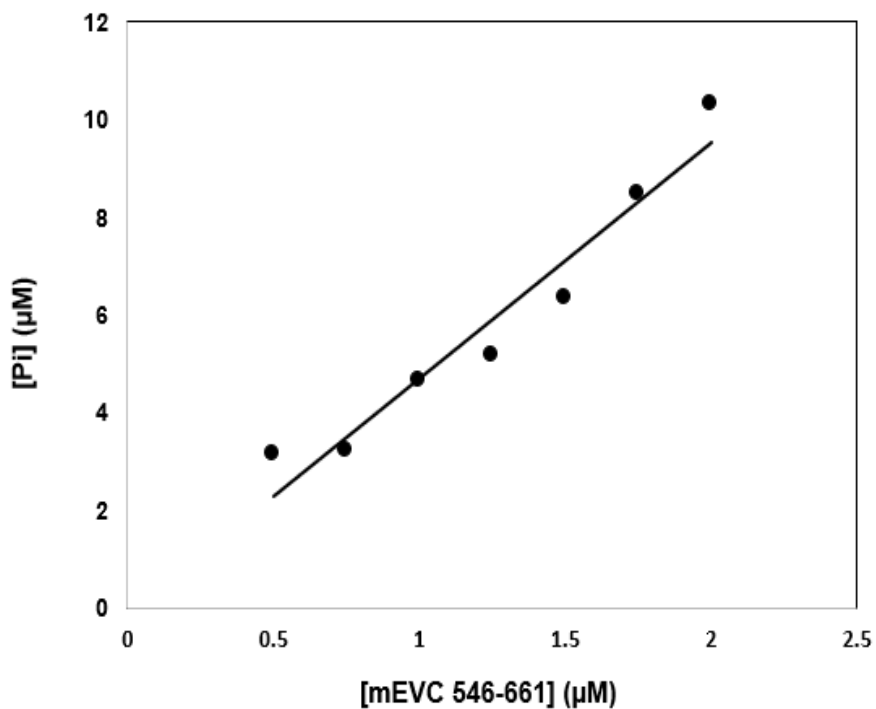


Figure 21. Optimal concentration of mEVC 546-661 for GTPase assay

3.5.4 Mouse EVC GTPase activity at varying concentrations of GTP

The potential GTPase activity of mouse EVC was assayed with increasing concentration of GTP, with and without pyrophosphatase. The GTPase activity of the protein increased as GTP concentration increased and remained essentially the same after 2 to 3 minutes. A plot of velocity versus GTP molar concentration showed that the enzyme displayed a typical Michaelis Menten hyperbolic curve (Figure 22). Velocity was determined as $\mu\text{M Pi}/\text{min}$.

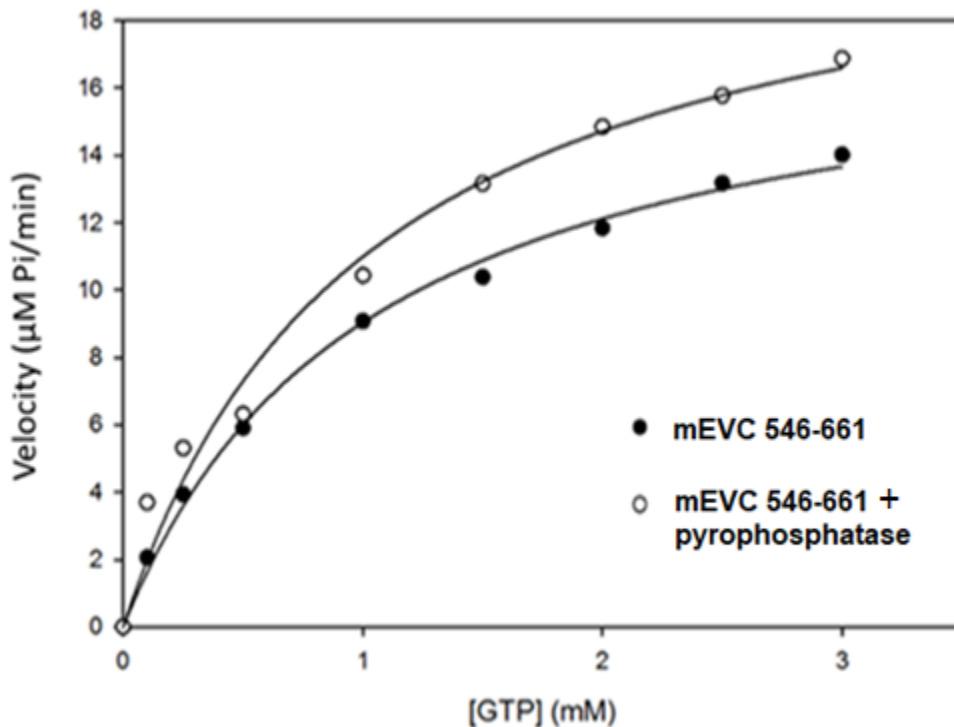


Figure 22. Michaelis-Menten plot of the GTP hydrolyzing activity of mouse EVC protein. GTPase activity was assayed using 2 μM of mouse EVC 546-661 protein in 300 μL total volume of buffer containing 50 mM Tris, pH 7.5, 1mM MgCl_2 , varying concentrations of GTP with or without 1 U of pyrophosphatase. Inorganic phosphate released was measured colorimetrically using a malachite-green dye assay at 650 nm. Activity was taken as micromolar inorganic phosphate released per unit time. All assays were performed at least in duplicates.

3.5.5 Hanes-Woolf plot for the GTPase activity of mEVC 546-661

Using the Hanes-Woolf modification of the Michaelis-Menten equation (equation 1), a plot of $[GTP]/V_o$ versus $[GTP]$ was made in the presence and absence of pyrophosphatase (Figures 23 A and B)

$$v = \frac{d[P]}{dt} = \frac{V_{\max}[S]}{K_M + [S]}$$

Equation 1. Michaelis–Menten equation

V_{\max} represents the maximum rate achieved by the system at saturating substrate concentration. The Michaelis constant K_M is the substrate concentration at which the reaction rate is half of V_{\max} .

The K_M and V_{\max} values were determined from the Hanes-Woolf plot (Figure 23). The kinetic parameters of mouse EVC GTP hydrolyzing activity are summarized in Table 5. k_{cat} is the turnover number or catalytic constant, defined as the number of times each enzyme site converts substrate to product per unit time. Turnover number- k_{cat} shows how fast ES complex proceeds to E + P and it is calculated using equation 2.

$$k_{\text{cat}} = V_{\max}/[ET]$$

Equation 2. Turnover number (k_{cat})

$[ET]$ is total enzyme concentration.

Catalytic efficiency (k_{cat}/K_M) reflects both binding and catalytic events, indicating how the velocity varies with the frequency of successful enzyme and substrate interaction.

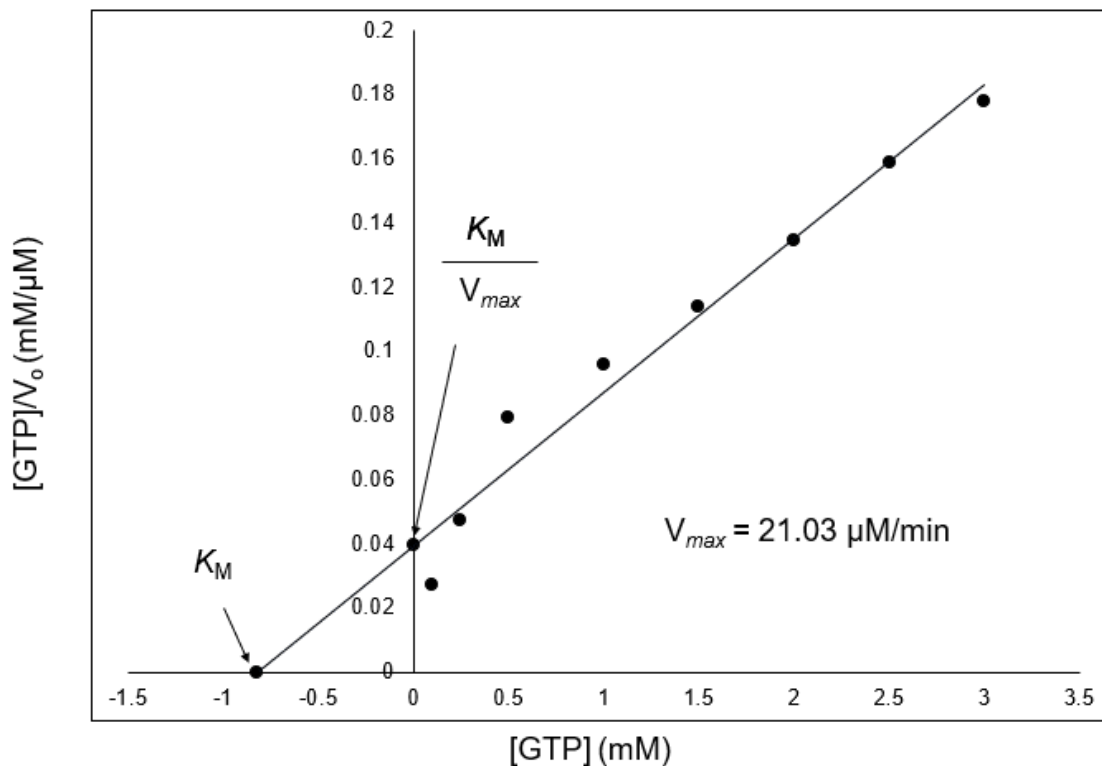


Figure 23. Hanes-Woolf plot of the GTP hydrolyzing activity of mEVC 546-661. Calculation of Michaelis-Menten constant (K_M) and maximum velocity (V_{max}) for mouse EVC GTPase activity at 2 μM enzyme were calculated.

Table 5. Kinetic parameters of mouse EVC 546-661 GTPase activity

Enzyme parameters	Calculated value
Specific activity ($\mu\text{moles}/\text{Pi}/\text{min}/\text{mg}$ enzyme)	6780
K_M	0.820
k_{cat} (sec^{-1})	0.175
Catalytic efficiency k_{cat}/K_M ($\text{M}^{-1}\text{sec}^{-1}$)	213

CHAPTER 4

DISCUSSION

Mutations in the *EVC* and/or *EVC2* genes are known to cause the Ellis-van Creveld syndrome and its milder form, Weyers acrofacial dysostosis (WAD). These mutations result in defective EVC and EVC2 proteins that disrupt the hedgehog signaling pathway causing developmental disorders such as malformed bones, teeth, nails, and polydactyly. To function, EVC and EVC2 proteins form a complex that interacts with a secondary receptor called Smo in the hedgehog signaling pathway. This multiprotein interaction also includes another protein complex, EFCAB7-IQCE, forming a protein assembly (39). Once formed, this multiprotein complex causes the dissociation of Gli3, a transcription factor, from its suppressor, Sufu and promotes its anterograde transport through the tip of the cilium.

Based on similar signaling pathways, it is believed that there is need for a source of energy to transduce the Hh signaling pathway, and to regulate its speed and amplitude. Several candidate proteins have been proposed for this role; however, no protein has been identified yet. Based on observations from bioinformatic analysis, the hypothesis of this study was that EVC protein was a GTPase that provided energy and served as an on/off switch for the Hh signaling pathway.

Mouse EVC was found to possess P-loop and leucine zipper motifs, which may be important for its function in the Hh signaling pathway. Multiple sequence alignment of EVC sequences from different animals using Clustal Omega, suggested that sequences of primate origins contain highly conserved P-loop motifs with the canonical consensus sequence, AxxxxGKS. However, the other animals, for example mouse contain less conserved P-loop motifs (AxxxxGQA in mouse). Mouse EVC (mEVC) P-loop lacks lysine, a basic, charged amino acid that forms hydrogen bond with β - and γ -phosphate groups of nucleotides. Instead of lysine, mEVC has glutamine, a charge-neutral, polar amino acid. Although lacking lysine, GTP binding site of mEVC may still preserve hydrogen bonding interactions with water or other molecules such as nucleotides due to free electron pairs of the amide groups in the side chain of the glutamine residue. However, the substitution of serine (a polar uncharged amino acid) for alanine (a nonpolar amino acid) may affect nucleotide binding and/or hydrolyzing activity of mEVC protein. Serine binds to β - and γ -phosphates by coordinating with the Mg^{2+} ion that balances negative charges of phosphate groups, and thus stabilizes the bound nucleotide. Having an alanine substituting for the otherwise highly conserved serine, results in complete loss of the hydroxyl group that mediates the Mg^{2+} -dependent stabilization of the bound nucleotide. The alanine cannot contribute in the same manner as the serine to the nucleotide binding.

Therefore, GTPase activity of mEVC may be affected by the degeneracy of its P-loop.

A second evidence emerged from the predicted 3D structure that supports the presence of a GTPase activity in EVC protein. The P-loop motifs in both mEVC and hEVC are exposed to the surrounding environment, thus making them accessible to solvated GTP. The presence of a leucine zipper motif opposite the P-loop may play a crucial role in the mechanism of EVC function. Leucine zipper is a protein–protein interaction motif consisting of a set of equidistant leucine residues within α -helices that are exposed for interaction with one another. Hence, homodimer conformation of EVC protein may be formed through the leucine zipper. Since leucine zipper is predicted at opposite site to P-loop, formation of dimer may not bury the active P-loop, thereby ensuring that GTP binding and hydrolyzing can still occur. However, it is proposed that the GTPase activity of EVC protein is influenced by dimerization and that this may regulate downstream hedgehog signaling pathway processes.

EVC and EVC2 physically interact in the cell and together regulate the hedgehog signaling pathway at the EVC zone (23). The predicted structure of EVC2, generated by RaptorX, revealed that the protein contains two putative “arginine finger” motifs; the first within the EVC-binding region (residues 250-671) and the other at a separate site. The first arginine finger motif (residues 250-671) is exposed to the surrounding environment, potentially able to make direct

bonding contacts with EVC. Arginine finger is a crucial motif required by GTPase activating proteins (GAPs). An arginine side chain (“finger”) is inserted into the active site of the GTPase enzyme, for example Ras, to stabilize the positioning of the catalytic glutamine and neutralize negative charges on the phosphates. Thus, the reaction rate of GAP-stimulated GTPase activity of Ras is increased by more than 4×10^4 fold than that of Ras by itself. Based on this observation, it is proposed that EVC2 stimulates the GTPase activity of EVC protein, likely in the same manner. Interestingly, the human EVC2 (hEVC2) possesses three arginine fingers, but only the first two motifs seem to be partially uncovered. The lack of exposure of the arginine fingers in hEVC2 suggests that they may not be accessible for interaction with the P-loop on hEVC. However, the P-loop of hEVC is highly conserved; therefore, hEVC may not require an arginine finger for optimal GTPase activity.

To study its GTPase activity, two fragments of the EVC protein, mEVC 546-661 and mEVC 285-627, were purified. While mEVC 546-661 contains both P-loop and leucine zipper, mEVC 285-625 possesses only P-loop. hEVC 546-661 was also purified and tested for its suspected GTPase activity. Plasmid constructs were designed to express EVC protein fragments that consisted of N-terminal (His)₆ tags which bind to Ni-NTA column. All the EVC protein fragments were insoluble in cell lysate; therefore, the proteins were purified in denaturing buffers by Ni-NTA agarose affinity. Ni-NTA affinity chromatography purification

yielded partially purified EVC proteins, so a reverse-gradient gel filtration was employed to obtain higher level of purity, refold the proteins and remove phosphate. The gradient gel filtration slowly removed urea and prevented precipitation of the refolding proteins. The final protein products were highly purified as confirmed by SDS-PAGE. EVC proteins could be concentrated up to 4 mg/ml after which they precipitated.

The intrinsic tryptophan fluorescence of the protein was used to test the suspected nucleotide-binding ability of EVC. mEVC protein produced high fluorescence intensity because it possesses a tryptophan residue close to the P-loop that is sufficiently exposed. In the presence of the GTP analog GppNHp, the fluorescence intensity was quenched drastically. It is assumed that binding of the analog caused conformational changes in the protein that occluded the fluorescence of the tryptophan residue. There was no difference in fluorescence intensity of mEVC 546-661 protein taken between 30 seconds and 2 minutes after binding the analog, but the intensity slightly increased 10 minutes after addition of the molecule. Fragment mEVC 546-661 contains both P-loop and leucine zipper. Notably, fluorescence quenching upon analog binding was less drastic in mEVC 285-627, a fragment lacking the leucine zipper. Also, there was clearly further decrease in fluorescence readings taken 30 seconds and 2 minutes after analog binding compared to mEVC 546-661. It took 2 minutes for quenching to peak in mEVC 285-627, while it took only 30 seconds in the case of

mEVC 546-661. This observation suggests that the leucine zipper motif in mEVC 546-661 influences GTP binding and/or hydrolyzing activity of the protein. However, in both proteins, the fluorescence started to recover 10 minutes after analog binding. It is possible that the proteins started to release the analog or its hydrolysis product and thus regain its fluorescence. Overall, these data indicate that mEVC protein is capable of binding GTP.

GTP hydrolyzing ability of EVC protein was tested by assaying for the generation of inorganic phosphate (Pi) when the nucleotide was added to solutions of the protein. Time-course GTP hydrolysis assay was carried out in the absence and presence of pyrophosphatase using fixed concentrations of EVC protein and the substrate, GTP. The mEVC 546-661 fragment, which contains both P-loop and leucine zipper released Pi from GTP hydrolysis when assayed alone. However, in the presence of pyrophosphatase, the amount of Pi released increased considerably. This observation suggests that mEVC 546-661 fragment releases both Pi and P₂ (the substrate for pyrophosphatase) from hydrolysis of GTP. Interestingly, the assay of fragment mEVC 285-627, which lacks leucine zipper, released P₂ when assayed alone, and Pi only in the presence of pyrophosphatase. These results indicate that mEVC 285-627 releases only P₂ from GTP hydrolysis. mEVC 285-627 lacks leucine zipper, and therefore the ability to dimerize. The protein exists only in the monomeric form as confirmed by SDS-PAGE. On the other hand, mEVC 546-661 exists as a mixture of the

monomeric and dimeric forms, even on SDS-PAGE. The implication of these data is that in its monomeric form, EVC protein hydrolyses GTP to GMP + PPi (pure GTPase) while in the mixed form, it generates GMP + PPi and GTP + Pi (mixed GTPase).

The time-course GTP hydrolysis assay was repeated using human EVC 546-661 (hEVC 546-661) in the absence and presence of pyrophosphatase. The hEVC 546-661 fragment possesses a highly conserved P-loop and leucine zipper. Notably, hEVC 546-661 released more Pi than mEVC 546-661 even at considerably lower concentration. In addition, hEVC 546-661 also displayed a mixed GTPase activity as observed in mEVC. The observed experimental data corroborated observations from bioinformatic analysis in several ways. First, that the presence of P-loop in EVC protein confers ability to bind and hydrolyze GTP. Second, that the presence of leucine zipper in EVC allows the protein to dimerize, and this dimerization affects its GTPase activity. Third, that the degeneracy of the P-loop in mouse EVC makes the protein less effective in GTP binding and/or hydrolyzing compared to the human version.

Numerous factors affect enzyme kinetics, including purity and concentration of enzyme, substrate concentration, pH, temperature, inhibitors, and assay time. In this study, concentration of enzyme and substrate as well as assay time were considered. As mEVC concentration was kept constant at 2 μ M, increasing the substrate concentration gradually led to increase in reaction rate

(Pi released per minute) until a maximum velocity V_{\max} , was reached. Michaelis-Menten plot of the GTP hydrolyzing activity (mixed GTPase) of mouse EVC protein was constructed. The K_M for GTP hydrolysis by mouse EVC (mEVC) was calculated to be 0.820 mM (or 820. μ M) from a Hanes-Woolf plot. A small K_M indicates high binding affinity of enzyme to substrate since the reaction can reach half of V_{\max} at low substrate concentration, and vice-versa. The turnover number, k_{cat} , for mEVC GTPase activity, was determined to be 0.175 sec^{-1} (or approximately 11.0 min^{-1}). The k_{cat} means the number of substrate molecules transformed by one active site of the enzyme per second.

The kinetic parameters obtained for the GTPase activity of EVC proteins were similar to those of large GTPases such as dynamin (40) and hGBP-1 (41). Structurally, dynamin possesses a GTP binding domain and an effector domain that stimulates its GTPase activity (40). Dynamin hydrolyzes GTP both as a monomer (basal form) and as a tetrameric assembly (40). The turn over numbers of the basal and assembly-stimulated GTPase activity of dynamin are 2.60 min^{-1} and 105 min^{-1} , respectively (40), suggesting that oligomerization influences its GTPase activity. The calculated k_{cat} for mEVC 546-661 (11.0 min^{-1}), is higher than that of monomeric dynamin (2.60 min^{-1}), but lower than that of tetrameric dynamin (105 min^{-1}). These observations suggest that the ability of mEVC 546-661 to dimerize via its leucine zipper somewhat influences its GTPase activity.

The human GBP-1, also a member of the dynamin superfamily of large GTPases, forms dimers or tetramers in solution, and this oligomerization is dependent on nucleotide binding. In the absence of nucleotide, hGBP-1 is in monomeric form, while the dimeric hGBP-1 is formed when bound to GppNHp (GTP analog) (41). It appears that EVC protein exists as a mixture of its monomeric and dimeric forms at a yet undetermined ratio. However, the presence of GTP may shift the ratio to favor the dimeric form of the protein, leading to preference for its $\text{GTP} \rightarrow \text{GDP} + \text{P}_i$ activity. Thus, EVC may be regarded as a large GTPase based on the similarities of its kinetic parameters to that of dynamin and hGBP.

The model in [Figure 24](#) is proposed to explain the relationship between the structure and GTPase activity of EVC. In the model, EVC in its monomeric form favors $\text{GTP} \rightarrow \text{GMP} + \text{PP}_i$ activity, while in its dimeric form favors $\text{GTP} \rightarrow \text{GDP} + \text{P}_i$ activity. In addition, dimerization of EVC is mediated by the leucine zipper motif in the protein, and this process may be promoted by the binding of GTP. This model could serve as a basis for future work.

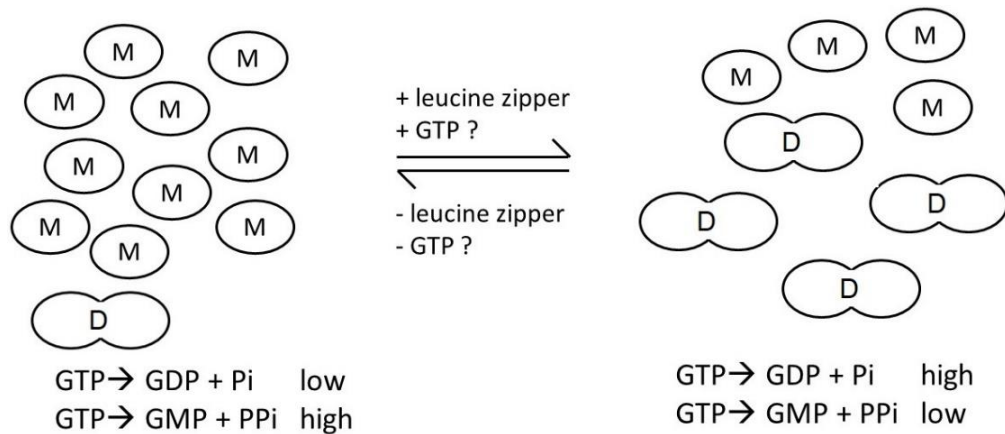


Figure 24. Proposed model for the relationship between the structure and GTPase activity of EVC. Leucine zipper, and possibly GTP, promote dimerization and/or oligomerization of EVC, shifting GTP hydrolysis from a mixture of $\text{GTP} \rightarrow \text{GMP} + \text{PPi}$ and $\text{GTP} \rightarrow \text{GDP} + \text{Pi}$ to predominantly $\text{GTP} \rightarrow \text{GDP} + \text{Pi}$.

M represents monomeric form of EVC. D represents dimeric form of EVC. Equation is not based on stoichiometric amounts of protein forms.

In conclusion, this work has provided the first experimental evidence to show that EVC protein possesses a measurable GTPase activity, and that dimerization of the protein via its leucine zipper motif influences this enzyme activity. Future experiments in this research work should include characterization of the GTPase activity of full-length EVC1 proteins, and further analysis of effect of dimerization on the GTPase activity of EVC proteins. In addition, the effects of EVC2 protein and common cofactors such as bivalent metals on the GTPase activity of EVC protein should be investigated.

REFERENCES

1. Das, D., Das, G., Mahapatra, T., and Biswas J. (2010) Ellis-van Creveld syndrome with unusual association of essential infantile esotropia. *Oman J. Ophthalmol.* **3**,23–25.
2. McKusick, V. A., Egeland, J. A., Eldridge, R., and Krusen, D. E. (1964) Dwarfism in the Amish I. The Ellis-Van Creveld syndrome. *Bull Johns Hopkins Hosp.* **115**,306–336.
3. Kamal, R., Dahiya, P., Kaur, S., Bhardwaj, R., and Chaudhary, K. (2013) Ellis-van Creveld syndrome: A rare clinical entity. *J. Oral Maxillofac. Pathol.* **17**,132–135.
4. Baujat, G., and Le Merrer, M. (2007). Ellis-Van Creveld syndrome. *Orphanet J. Rare Dis.* **2**,27.
5. Shi, L., Luo, C., Ahmed, M. K., Attaie, A. B., and Ye, X. (2016). Novel mutations in *EVC* cause aberrant splicing in Ellis–van Creveld syndrome. *Mol. Genet. Genomics.* **291**,863–872.
6. TCGA Research Network. <https://www.cancer.gov/tcga>.
7. Polymeropoulos, M., Ide, S., Wright, M., Goodship, J., Weissenbach, J., Pyeritz, R., Da Silva, E., Ortiz De Luna, R. and Francomano, C. (1996). The Gene for the Ellis–van Creveld Syndrome Is Located on Chromosome 4p16. *Genomics.* **35**,1-5.

8. Ruiz-Perez, V., Ide, S., Strom, T., Lorenz, B., Wilson, D., Woods, K., King, L., Francomano, C., Freisinger, P., Spranger, S., Marino, B., Dallapiccola, B., Wright, M., Meitinger, T., Polymeropoulos, M. and Goodship, J. (2000). Mutations in a new gene in Ellis-van Creveld syndrome and Weyers acrodistal dysostosis. *Nature Genetics*. **24**, 283-286.
9. Ruiz-Perez, V., Stuart Tompson, W., Helen Blair, J., Espinoza-Valdez, C., Lapunzina, P., Silva, E., Hamel, B., Gibbs, J., Young, I., Wright, M. and Goodship, J. (2003). Mutations in Two Nonhomologous Genes in a Head-to-Head Configuration Cause Ellis-van Creveld Syndrome. *Am. J. Hum. Genet.* **72**, 728-732.
10. Galdzicka, M., Patnala, S., Hirshman, M., Cai, J., Nitowsky, H., A Egeland, J., and Ginns, E. (2002). A new gene, EVC2, is mutated in Ellis–van Creveld syndrome. *Mol. Genet. Metab. Rep.* **77**, 291-295
11. Sund, K., Roelker, S., Ramachandran, V., Durbin, L., and Benson, D. (2009). Analysis of Ellis-van Creveld syndrome gene products: implications for cardiovascular development and disease. *Hum. Mol. Genet.* **18**, 1813-1824.
12. Saraste, M., Sibbald, P., and Wittinghofer, A. (1990). The P-loop — a common motif in ATP- and GTP-binding proteins. *Trends Biochem. Sci.* **15**, 430-434.
13. Liu, S., Dontu, G., and Wicha, M. (2005). Mammary stem cells, self-renewal pathways, and carcinogenesis. *Breast Cancer Res.* **7**, 86-95.

14. Bokoch, G. (2005) Regulation of innate immunity by Rho GTPases. *Trends Cell Biol.* **15**, 163–171.
15. Sot, B., Behrmann, E., Raunser, S., and Wittinghofer, A. (2012). Ras GTPase activating (RasGAP) activity of the dual specificity GAP protein Rasal requires colocalization and C2 domain binding to lipid membranes. *Proc. Natl. Acad. Sci. U.S.A.* **110**, 111-116.
16. Garcia de Viedma, D., Giraldo, R., Rivas, G., Fernández-Tresguerres, E. and Diaz-Orejas, R. (1996). A leucine zipper motif determines different functions in a DNA replication protein. *EMBO J.* **15**, 925-934.
17. Miller, M., Shuman, J. D., Sebastian, T., Dauter, Z., and Johnson, P. F. (2003) Structural Basis for DNA Recognition by the Basic Region Leucine Zipper Transcription Factor CCAAT/Enhancer-binding Protein. *J. Biol. Chem.* **278**, 15178–15184.
18. Abdullah, N., Balakumari, M., and Sau, A. K. (2010). Dimerization and Its Role in GMP Formation by Human Guanylate Binding Proteins. *Biophys. J.* **99**, 2235–2244.
19. The UniProt Consortium (2019) UniProt: a worldwide hub of protein knowledge. *Nucleic Acids Res.* **47**, D506-515
20. Blair, H. J., Tompson, S., Liu, Y. N., Campbell, J., MacArthur, K., Ponting, C. P., Ruiz-Perez, V. L., and Goodship, J. A. (2011). Evc2 is a positive

- modulator of Hedgehog signalling that interacts with Evc at the cilia membrane and is also found in the nucleus. *BMC Biol.* **9**,14.
21. Kötting, C., Kallenbach, A., Suveyzdis, Y., Wittinghofer, A., and Gerwert, K. (2008) The GAP arginine finger movement into the catalytic site of Ras increases the activation entropy. *Proc. Natl. Acad. Sci. U.S.A.* **105**, 6260–6265.
22. Jia, Y., Wang, Y., and Xie, J. (2015) The Hedgehog pathway: role in cell differentiation, polarity and proliferation. *Arch Toxicol* **89**, 179–191.
23. Nozawa, Y. I, Lin, C., and Chuang, P. T. (2013) Hedgehog signaling from the primary cilium to the nucleus: an emerging picture of ciliary localization, trafficking and transduction. *Curr. Opin. Genet. Dev.* **23**, 429–437.
24. Ruiz-Perez, V. L., Blair, H. J., Rodriguez-Andres, M. E., Blanco, M. J., Wilson, A., Liu, Y. N., Miles, C., Peters, H., and Goodship, J. A. (2007). Evc is a positive mediator of Ihh-regulated bone growth that localises at the base of chondrocyte cilia. *Development.* **134**,2903-12.
25. Hills, C. B., Kochilas, L., Schimmenti, L. A., and Moller, J. H. (2011). Ellis–van Creveld Syndrome and Congenital Heart Defects: Presentation of an Additional 32 Cases. *Pediatr. Cardiol.* **32**, 977–982.
26. Caparrós-Martín, J. A., Valencia, M., Reytor, E., Pacheco, M., Fernandez, M., Perez-Aytes, A., Gean, E., Lapunzina, P., Peters, H., Goodship, J. A., and Ruiz-Perez, V. L., (2013). The ciliary Evc/Evc2 complex interacts with

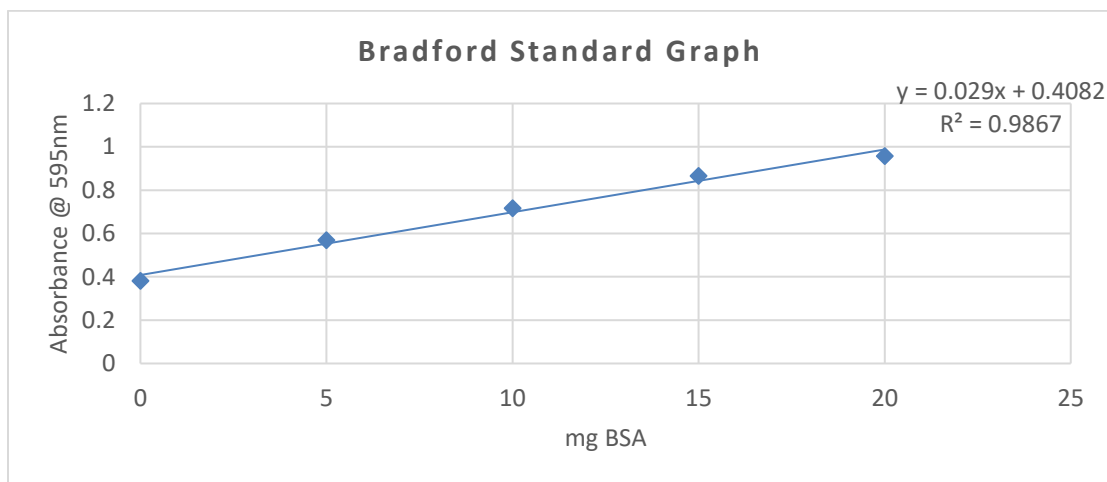
- Smo and controls Hedgehog pathway activity in chondrocytes by regulating Sufu/Gli3 dissociation and Gli3 trafficking in primary cilia. *Hum. Mol. Genet.* **22**, 124–139
27. Takahashi, R., Yamagishi, M., Nakano, K., Yamochi, T., Yamochi, T., Fujikawa, D., Nakashima, M., Tanaka, Y., Uchimaru, K., Utsunomiya, A., and Watanabe, T. (2014) Epigenetic deregulation of Ellis-van Creveld confers robust Hedgehog signaling in adult T-cell leukemia. *Cancer Sci.* **105**, 1160–1169
28. Rubin, L. L., and de Sauvage, F. J. (2006) Targeting the Hedgehog pathway in cancer. *Nat. Rev. Drug Discov.*, **5**, 1026–1033.
29. Odunuga, O. O., Adekoya, O. A., and Sylte, I. (2015) High-level expression of pseudolysin, the extracellular elastase of *Pseudomonas aeruginosa*, in *Escherichia coli* and its purification. *Protein Expr. Purif.* **113**, 79-84.
30. Monsivais, A. (2010). Expression, partial purification and biochemical characterization of mouse EVC protein. master's thesis, Stephen F. Austin State University.
31. Chojnacki, S., Cowley, A., Lee, J., Foix, A., and Lopez, R. (2017) Programmatic access to bioinformatics tools from EMBL-EBI
32. Källberg, M., Wang, H., Wang, S., Peng, J., Wang, Z., Lu, H., and Xu, J. (2012) Template-based protein structure modeling using the RaptorX web server. *Nat. Protoc.* **7**, 1511-1522.

33. Ma, J., Peng, J., Wang, S., and Xu, J. (2012) A Conditional Neural Fields model for protein threading. *Bioinformatics*. **28**, 59-66.
34. Ma, J., Wang, S., Zhao, F., and Xu, J. (2012) Protein threading using context-specific alignment potential. *Bioinformatics*. **29**, 257-265.
35. Peng, J., and Xu, J. (2011) A multiple-template approach to protein threading. *Proteins*. **79**, 1930-1939.
36. Peng, J., and Xu, J. (2011) RaptorX: exploiting structure information for protein alignment by statistical inference. *Proteins*. **79**, 161-171.
37. Pettersen, E. F., Goddard, T. D., Huang, C. C., Couch, G. S., Greenblatt, D. M., Meng, E. C., and Ferrin, T. E. (2004) UCSF Chimera - A Visualization System for Exploratory Research and Analysis. *J. Comput. Chem.* **25**, 1605-1612
38. Ennion, S., Hagan, S., and Evans, R. J. (2000) The role of positively charged amino acids in ATP recognition by human P2X1 receptor. *J. Biol. Chem.* **10**, 35656
39. Pusapati, G. V., Hughes, C. E., Dorn, K. V., Zhang, D., Sugianto, P., Aravind, L., Rohatgi, R. (2014) EFCAB7 and IQCE regulate hedgehog signaling by tethering the EVC-EVC2 complex to the base of primary cilia. *Dev. Cell* **28**, 483-496.

40. Song, D. B., Leonard, M. L., and Schmid, L. S. (2004). Dynamin GTPase Domain Mutants That Differentially Affect GTP Binding, GTP Hydrolysis, and Clathrin-mediated Endocytosis. *J. Biol. Chem.* **279**, 40431–40436.
41. Prakash, B., Praefcke, G. J. K., Renault, L., Wittinghofer, A., and Herrmann, C. (2000a) Structure of human guanylate-binding protein 1 representing a unique class of GTP-binding proteins. *Nature.* **403**, 567–571.

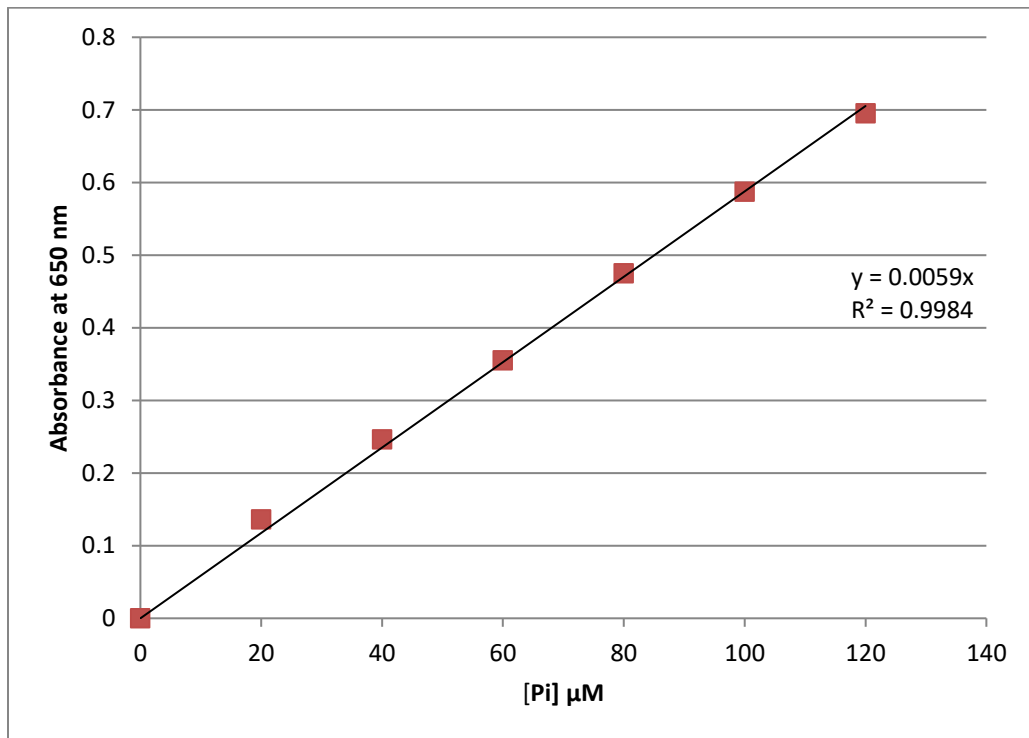
APPENDIX A

Protein concentration were determined using the Bradford colorimetric assay. A linear standard graph generated using varying concentrations of bovine serum albumin (BSA) was used to extrapolate absorbance value into protein concentration and used to determine the concentrations of purified proteins.



APPENDIX B

PHOSPHATE STANDARD CURVE



VITA

After completing her work at Nguyen Huu Huan high school, Ho Chi Minh, Vietnam, in 2007, Giang Thi Huong Nguyen entered the International University at Ho Chi Minh, Vietnam. She received the degree of Bachelor of Science from International University in 2012. In September 2017, she entered the Graduate School of Stephen F. Austin State University, Nacogdoches, TX and received the degree of Master of Science in May of 2019.

Permanent Address: 13526 Dahlia Greenway
 Houston, TX77038

Style followed for citing references: Journal of Biological Chemistry

This thesis was typed by Giang Thi Huong Nguyen in May 2019.